- 1 This is a non-peer reviewed manuscript preprint submitted
- 2 to EarthArXiv. This paper has been submitted to the Journal
- **of the Geological Society of London. The authors welcome**
- 4 feedback on this article.

5

- 6 A new source-to-sink synthesis of the Middle Triassic
- 7 Helsby Sandstone Formation (Sherwood Sandstone Group)
- 8 river systems in the British Isles

9

10 Xiang Yan*, Gary J. Hampson & Alexander C. Whittaker

11

- 12 Department of Earth Science and Engineering, Imperial College London, London SW7 2AZ,
- 13 *UK*
- 14 *Correspondence: Xiang.yan19@imperial.ac.uk

15

Abstract

16

17

18

19

20

21

22

23

24

25

26

27

28

29

30

31

32

Sediment grain size and mineralogy change in sediment routing systems from source to sink. A better understanding of sediment routing allows improved predictions to be made of the bulk grain-size and mineralogy of sandstone fairways. We present a new appraisal of sediment routing in the Triassic Helsby Sandstone Formation (Sherwood Sandstone Group) and lowermost Mercia Mudstone Group of the British Isles, which constitute a key play for geological sequestration of CO2. These strata were deposited and supplied by a major, northflowing river system, which is traced from its source region in north France to beyond the Irish Sea. We construct a new, integrated litho- and chronostratigraphic model to correlate key units across the British Isles. We then present sediment isopachs and volumes for this chronostratigraphic interval, and resolve paleogeographic discrepancies using published sedimentological datasets, supplemented by a new synthesis of bulk sandstone mineralogy. Finally, we present a unified, updated sediment routing map for the Helsby Sandstone Formation. Importantly, differences in bulk sandstone mineralogy between the south and north of the studied fairway signifies that aside from its primary source area in France, substantial tributaries modified the composition of the Helsby Sandstone Formation along the course of the sediment routing system.

33

34

35

36

37

38

39

40

Introduction

Sediment transport via rivers is a key surface process that transfers mass from areas of uplift and erosion to depocentres, i.e. from sediment sources to sediment sinks. Source-to-sink systems can be divided into segments: areas of uplift and erosion where sediment is generated, areas of sediment bypass and transient storage, and subsiding depocentres that serve as the main sediment sinks (e.g. Somme et al., 2009; Romans and Graham, 2013; Helland-Hansen et al., 2016). The size, shape and distribution of sediment routing systems

are controlled by their geomorphology (e.g. Somme et al., 2009; Helland-Hansen et al., 2016; Markwick, 2019), which is seldom completely preserved over deep time (Romans and Graham, 2013; Helland-Hansen et al., 2016). Consequently, reconstructing an accurate palaeogeography is essential for constraining source-to-sink sediment routing in the geological record (e.g. Markwick, 2019; Wrobel-Daveau et al., 2022). Understanding source-to-sink sediment routing is in turn a crucial tool to evaluate landscape responses to climate change and tectonics, as well as for predictive resource exploration (Wrobel-Daveau et al., 2022; Castelltort et al., 2023).

Source-to-sink sediment routing is commonly constrained by several methods, and involves the integration of lithostratigraphy, chronostratigraphy, and palaeogeography, the latter constrained by methods including quantitative provenance analysis, sedimentology and palaeocurrents (e.g. Morton and Hallsworth, 1993; Hampson et al., 2014; Helland-Hansen et al., 2016; Michael and Zuhlke, 2022; Castellort et al., 2023). Synthesising these data can produce a defined stratigraphy and age model, sediment volumes, and a defined map of sediment source areas and sinks.

In this study, we focus on the Triassic Sherwood Sandstone Group (SSG) of the British Isles: a predominantly fluvial, regionally important sediment routing system, dated c. 249-240 Ma (fig. 1a, Hounslow and McIntosh, 2003; Hounslow and Gallois, 2023). The SSG was deposited at low latitudes of about 20° N during the early breakup of Pangea (fig. 1b), and in the aftermath of the Permo-Triassic extinction (Radley and Coram, 2016; Newell, 2018a; b). Much of the SSG is interpreted to have been laid down by major, north-flowing river systems that originated from Variscan highlands, now situated in northern France (fig. 1c, e.g. Wills, 1956; Burley, 1987; Tyrrell et al., 2012; Morton et al., 2016; Newell, 2017a; Burgess et al., 2024). The SSG has served as a key target for hydrocarbon exploration and production (e.g. Cowan, 1993; McKie et al., 1997, Floodpage et al., 2001; Medici et al., 2019a; Scorgie et al., 2021), for geothermal energy production (Downing et al., 1983; Knox et al., 1984), and is a key groundwater aquifer (Plant et al., 1999; Newell and Smith, 2009; Medici et al., 2019b).

More recently, the SSG has also become a key target for geological sequestration of CO₂ (e.g. Holliday et al., 1991; Newell and Shariatipour, 2016; Scorgie et al., 2021; Chedburn et al., 2022; English et al., 2024; Gibson-Poole et al., 2025; Head et al., 2025). The SSG transitioned into the Mercia Mudstone Group (MMG), which forms the sealing unit for the SSG reservoir during the mid-Triassic (**fig. 1a**, e.g. McKie et al., 1997; Scorgie et al., 2021; Chedburn et al., 2022; English et al., 2024 Hounslow and Gallois, 2023).

The most recent palaeogeography, published more than 30 years ago (fig. 1c, Warrington and Ivimey-Cook, 1992), describes a major north-flowing sediment routing system flowing from the remnant Variscan highlands of north France, through a series of linked extensional basins in the UK, of the East Irish Sea Basin (EISB). This follows the older palaeogeographic interpretations from Wills (1970), Audley-Charles, (1970b), and Burley (1987). However, unlike previous interpretations, there is no mention or depiction of lateral sediment inputs, and sediment routing in the Wessex Basin and beyond the EISB remains unclear. Furthermore, the SSG-MMG transition is poorly understood. Finally, the paleogeographic extent of the catchments which sourced the fluvial systems of the SSG remain poorly constrained, as is their relation to the wider paleogeography of NW Europe.

Integration of data and research that has become available since the publication of Warrington and Ivimey-Cook (1992) could help to reconcile these uncertainties and knowledge gaps: For instance subsequent regional studies on the British Triassic system have collected and synthesised existing information to build basin-scale depositional models (e.g. Hamblin et al., 1992; Jackson et al., 1995; Plant et al., 1999; Dunford et al., 2001; Newell, 2018b; 2023; Marsh et al., 2022) while quantitative provenance analysis (Tyrrell et al., 2012; Morton et al., 2013; 2016) has provided higher resolution constraints on sediment source areas and sediment routing within the SSG. At the same time, better characterisation of the pre-Triassic basement allows inferences to be made about source area composition (e.g. Baptiste, 2016; Butler, 2018). Emerging chronostratigraphy has allowed the improved correlation of coeval units both across the UK (Mange et al., 1999; 2007; Hounslow and McIntosh, 2003; Hounslow

et al., 2017; Houslow and Gallois, 2023), and to the wider European Triassic system (Bourquin et al., 2011, McKie, 2017). Lastly, improved understanding of the early Triassic climate (Péron et al., 2005; Ravidà et al., 2021) and tectonics (Newell, 2018a) have offered further insights into controls on sediment generation.

In summary, the last 30 years of research has resulted in a situation in which the SSG and MMG of the British Isles is locally well-characterised in many aspects, yet is poorly resolved on the scale of the sediment routing system. Consequently, the aim of this paper is to produce a comprehensive, up-to-date and quantitative reconstruction of this source-to-sink system, harmonised with the palaeogeography of northwest Europe. To this end, we develop a unified lithostratigraphic and chronostratigraphic synthesis of key units in the SSG and MMG, focussing on a well-defined chronostratigraphic interval consisting of the upper SSG and lower MMG, in which the sediment routing system is well constrained. We then present new maps of the sediment fairway using standardised nomenclature compiled from previous palaeogeographic studies. Using these products as a framework, we present the first quantitative estimates of the volume and distribution of fluvial and aeolian deposits within the fairway. We then present isopach maps and volumes for units of interest. We then synthesise downsystem trends in sediment composition and provenance to characterise source-to-sink sediment routing, as well as the composition and extent of source areas. finally, we use these data to evaluate the size and position of sediment inputs into the sediment routing system.

Geological framework

The British Triassic system begins during the lower Triassic with the SSG (Hounslow and McIntosh, 2003), and passes into the MMG during the mid-Triassic (**fig. 1a**, Hounslow and Gallois, 2023). Deposition occurred in a series of linked, N-S trending extensional basins throughout the UK, spanning the area between the English Channel and the Irish Sea (Warrington and Ivimey-Cook, 1992).

The standardised lithostratigraphy of the SSG, defined by the British Geological Survey (BGS, Ambrose et al., 2014), divides the group into three formations based on a sequence typified in the Cheshire Basin. These three formations are the conglomeratic and sandy fluvial Chester Formation (CHF), the mixed fluvial-aeolian Wilmslow Sandstone Formation (WSF) and the fluvial-aeolian Helsby Sandstone Formation (HSF) (fig. 2; Ambrose et al., 2014; Newell, 2018a). Deposition of the HSF in the Wessex Basin and Worcester Graben was partially contemporaneous with the deposition of the lowermost MMG in the Cheshire Basin and EISB (fig. 1a, c). The stratigraphy of the lower MMG is similarly standardised (Howard et al., 2008), and is represented by the Tarporley Siltstone Formation (TSF) and the Sidmouth Mudstone Formation (SMF) (fig. 2; e.g. Warrington et al., 1970b; Wilson, 1990; 1993; Newell, 2018a).

The BGS standardised stratigraphy supersedes older stratigraphic terminology which differed between sedimentary basins (**fig. 2**). Unit names for basin-level stratigraphy are presented in **Figure 2**, based on the synthesis of Ambrose et al. (2014) and Howard et al. (2008). The older, basin-scale terminology is still widely used (e.g. Newell, 2018a; b; Scorgie et al., 2021; Marsh et al., 2022; Chedburn et al., 2022), but must be placed in the context of the wider source-to-sink system, which is best represented using the standardised BGS stratigraphy (**fig. 2**).

The CHF (**fig. 1a**) was laid down during the lower Triassic by a long-distance fluvial system sourced from the remnant Variscan mountains in north France (e.g. Tyrrell et al., 2012; Morton et al., 2013; 2016). The river system flowed northwards into the East Irish Sea Basin, possibly reaching Northern Ireland (Franklin et al., 2020; Moscardini et al., 2025). Deposition during the CHF is thought to have occurred in an extreme and variable semi-arid climate during the aftermath of the Permo-Triassic extinction, resulting in its abnormally coarse grain size (Radley and Coram, 2016; Newell, 2018a).

The overlying WSF is conformable over the CHF (figs. 1a, 2), and is thought to represent a period of dominantly aeolian activity caused by a accelerated extensional faulting.

resulting in the disconnection of basins and dissection of the SSG fairway (Newell, 2018a). The boundary between the WSF and the overlying HSF is largely disconformable (**fig. 2**), representing a period of tectonic uplift traditionally attributed to the Europe-wide Hardegsen tectonic event (Evans et al., 1993; Mange et al., 1999; 2007; Bourquin et al., 2011).

The HSF (**fig. 1a**) represents a second, mid-Triassic interval of fluvial activity (Newell, 2017a; b). HSF deposition is thought to have occurred in a more stable, albeit still semiarid climate (Newell, 2018) coinciding with a biotic recovery (Benton and Spencer, 2002; Coram et al., 2019). The mid-Triassic then saw a gradual aridification, with the river systems of the HSF retreating southwards. Fluvial-aeolian deposition was replaced by the playa lakes and marine evaporites of the MMG (**fig. 1a**, e.g. Greenwood and Habesch, 1991; Jackson et al., 1995; Plant et al., 1999; McKie, 2017) until fluvial activity finally ceased in the Wessex Basin (Newell, 2018b; Hounslow and Gallois, 2023).

Deposition of the CHF and HSF has previously been attributed to the 'Budleighensis' River (sensu Wills, 1956; 1970; 1976), a major (>350km) river system sourced from the Variscan-Cadomian massifs of northern France (Tyrrell et al., 2012; Morton et al., 2013; 2016). However, substantial changes in sediment mineralogy are known to occur downsystem between the Wessex Basin and the East Irish Sea Basin (**fig. 1c**, Burley, 1987; Plant et al., 1999; Morton et al., 2013), and it remains unclear how important the Gallic Massif source area was for the sediment routing system, relative to other potential sediment inputs further north.

In the context of northwest Europe, the north-flowing 'Budleighensis' system which deposited the SSG shares a Variscan-Cadomian Gallic Massif source area (sensu Sass et al., 2023) with two other substantial fluvial systems: an east-flowing system which deposited the Buntsandstein in France and Germany (the 'Alemania' *sensu* Ravidà et al., 2021), and a southeast-directed system which deposited the Buntsandstein in Iberia (e.g. Sanchez Martínez et al., 2012; Bourquin et al., 2011; McKie, 2017). The Gallic Massif was an upland region covering much of north France, encompassing the modern-day Armorican Massif, the

French Massif Central and the buried Variscan-Cadomian basement surrounding them, under the Paris Basin and English Channel.

The SSG exists in tectonostratigraphic continuity with underlying Permian aeolian sandstones and playa lake mudstones, which represent the first significant basin fill after the collapse of the Variscan Orogeny (e.g. Hamblin et al., 1992; Jackson et al., 1995; Newell, 2018a), as well as the overlying Mercia Mudstone Group (e.g. Howard et al., 2008; Hounslow et al., 2017; McKie, 2017). The post-depositional history of the SSG is variable between basins, however the unit has generally undergone 2-4 km of burial across the UK (e.g. Carter et al., 1995; Mikkelsen and Floodpage, 1997; Bray et al., 1998; Carter et al., 2001; Pharaoh et al., 2018). The northern section of the SSG fairway, particularly in NW England and offshore in the Irish Sea, has additionally seen substantial exhumation and erosion during the Cenozoic, bringing the SSG to outcrop (e.g. Mikkelsen and Floodpage, 1997; Pharaoh et al., 2018).

Overall, several uncertainties remain in characterising the SSG of the British Isles. The chronostratigraphy of the SSG and lower MMG is not rigorously integrated with the existing lithostratigraphy across the British Isles. The sediment fairway must be mapped out, and sediment volumetrics must be quantified. Variations in bulk sandstone mineralogy must be appraised down the sediment fairway. Sediment routing must be mapped out to reconcile the uncertainties presented previously. Finally, source areas must be reappraised using updated, published data. We seek to address these uncertainties in this study.

Methods

A synthesis of the lithostratigraphy of the HSF, TSF and lower SMF was completed to allow for a correlation of units between sedimentary basins in the British Isles. Chronostratigraphy was synthesised using the magnetostratigraphically constrained section of the HSF in the Wessex Basin (Hounslow and McIntosh, 2003; Hounslow and Gallois, 2023), and an equivalent section in the EISB (Hounslow and McIntosh, 2003; Mange et al., 1999).

which was then correlated to the global Triassic timescale (Ogg et al., 2020). These sections are then supplemented by published palynology, and the correlation of lithostratigraphic units and boundaries across the HSF, TSF and lower SMF. From this litho- and chronostratigraphic model, a single, time-equivalent interval within the sediment fairway could then be defined for analysis. This studied interval represents 5 Myr, from 246.5 Ma to 241.5 Ma, as detailed later.

To map the fairway of this chronostratigraphically defined interval, a geological database was compiled from published outcrop sections and borehole logs, and borehole records held by the BGS Onshore Single Borehole Index (SOBI), the Bureau de Recherches Géologiques et Minières (BRGM), the UK Onshore Geophysical Library (UKOGL), and the North Sea Transition Authority (NSTA) National Data Repository (NDR), as shown in **Figure 3**. For all data points (n = 393), lithostratigraphic units, thicknesses and dominant lithologies were recorded. In areas where data points were too dense to manually parse or where sources offered contradictory interpretations, published interpretations were prioritised. In the absence of any existing interpretations, original interpretations were made using wireline logs and lithological data. Where data were sparse or absent, or where the SSG was absent due to post-depositional erosion, the fairway was mapped based on existing palaeogeographic interpretations.

The resulting sediment fairway map was then integrated with nomenclature for sedimentary basins, palaeohighs and major structural features from existing palaeogeographic reconstructions (e.g. Wills, 1956; 1970, Audrey-Charles, 1970b; Burley, 1987; Warrington and Ivimey-Cook, 1992; Bourquin et al., 2011; Newell, 2018a) to create a full palaeogeographic framework for the middle Triassic of the British Isles. Our reconstruction further addresses major unknowns in fairway extent, and reconciles inconsistencies between previous interpretations.

Where the sediment fairway was sufficiently constrained by thickness data (**fig. 3**), stratigraphic thicknesses were combined with a series of points with zero stratigraphic thickness (n = 32), representing the bounds of nondeposition around Triassic massifs from the

palaeogeographic framework. These points were collectively interpolated with a regional fault map based on BGS data (DiGRock250k, 2008; 2013) and Newell (2017b) to produce isopach maps for each studied lithostratigraphic unit. Resulting sedimentary rock volumes were then computed for each basin. These volumes were then converted to solid rock volumes by removing pore space, a parameter well-constrained by previous studies.

The volume of fluvial and aeolian deposits in the HSF for each basin was estimated by assessing basin-scale sedimentological trends synthesised from literature. Estimates of the proportion of fluvial deposits by basin for the HSF were calculated by Medici et al. (2019a). However, these estimates were limited to outcrop observations and are therefore biased to basin margin locations. Furthermore, as their method of calculation is not explicit, it is challenging to verify the estimates of Medici et al. (2019a) directly. Consequently, we provide new estimates for the proportion of fluvial deposits based on large-scale sedimentological trends defined by outcrop and borehole data across each basin. The fluvial deposit contents of fluvial-dominated successions and aeolian-dominated successions are assumed to be 100% and 0%, respectively. The fluvial deposit content of fluvio-aeolian sequences is set at 50%.

Petrographic data for bulk sandstone mineralogy in the HSF was compiled from 7 sources across 16 localities in the sediment fairway, resulting in 320 data points (Ali, 1982; Knox et al., 1984; Burley, 1987; Chisholm et al., 1988; Svendsen and Hartley, 2001; Scorgie et al., 2021; De Sainz Simpson, 2022; Meadows, pers. Comms, see **supplementary material 2 for full dataset**). Owing to the historic differences in point counting methodology (e.g. Garzanti, 2019; Augustsson, 2021), these data cannot be compared as a single group but must be divided into two groups based on the point count definition of rock fragments.

The Indiana method of point counting (e.g. Basu, 1976) assigns all lithic fragments to the 'L' pole. The Gazzi-Dickinson method (Ingersoll et al., 1984; Zuffa, 1985) considers fragments by their constituent mineral phase: sand-grade (>0.0625 mm) quartz and feldspar phases within lithic fragments are assigned to the 'Q' or 'F' pole; all other lithic components are assigned to the 'L' pole. For the same bulk mineralogical assemblage plotted on a QFL

diagram, the Indiana method results in a more diffuse clustering of points, generally closer to the 'L' pole, and the Gazzi-Dickinson method results in points which cluster tightly, and closer to the Q-F line (Augustsson, 2021). For some datasets, this information was provided by the authors. For other studies, point counting methods could be inferred based on the resultant QFL plot. For each point counting method, data was grouped by basin, and then separated by aeolian and fluvial deposits to characterise the bulk mineralogical variability of sandstones within the sediment fairway. Sediment mineralogy within the HSF has also been studied in the context of quantitative provenance analysis (e.g. Plant et al., 1999; Tyrrell et al., 2012; Morton et al., 2013; 2016). These studies are equally key in constraining sediment routing and source areas, and are discussed separately in the basin-by-basin synthesis of sediment routing (see below).

Although the bulk mineralogy of the lower MMG has also been studied in the sand fraction (Scorgie et al., 2021; De Sainz Simpson et al., 2022) and the silt-clay fraction (Jeans, 2006; Armitage et al., 2013; Jones et al., 2025), interpreting sediment routing in the MMG is problematic. There are no sediment provenance studies to support compositional data, and understanding of depositional environments in the MMG in Cheshire Basin and EISB remains limited. For the purposes of this study, we hence focus on sediment mineralogy in the HSF. A first-order synthesis of diagenesis was then compiled to assess its impact on detrital mineralogy. This was then generalised throughout the fairway by using a compilation of burial histories for each basin. From this, the detrital mineralogy of the HSF could be appraised, and the downsystem variability of bulk sandstone mineralogy could be assessed.

Basin-by-basin sediment routing in the HSF fairway was then established. Existing, basin-scale studies characterising the HSF were combined with representative palaeocurrent indicators and quantitative provenance analysis recorded from published literature, and our synthesis of sediment mineralogy. From this, we inferred sediment routing directions, additional sediment inputs into the system, and where present, the degree of fluvial-aeolian

interaction. Data from each basin were then linked to provide a record of sediment routing within the whole HSF fairway.

Using the previously developed palaeogeographic and sediment routing framework, emergent uplands across northwest Europe were then lithologically and, where possible, palaeotopographically characterised. Sediment routing for the HSF was then integrated with existing constraints on sediment routing in northeastern Iberia and northwest Europe to produce a reconciled map of sediment sourcing. By constraining the extent and coverage of non-preserved drainage in the source areas of the HSF, the source-to-sink system could be fully characterised.

Stratigraphy

Revised terminology

Table 1 contains a list of commonly abbreviated stratigraphic and geographic terms. The 'Budleighensis River' (sensu Wills, 1956) was conceived as the main, north-flowing river which brought the distinctive quartzite clasts of the CHF from a southern Variscan source area into the Midlands. Since then, the term 'Budleighensis River' has been expanded to encompass all fluvial activity occurring within the CHF and HSF (e.g. Plant et al., 1999; Tyrrell et al., 2012; Radley and Coram, 2016; Newell, 2018; Franklin et al., 2020; Burgess et al., 2024). This is problematic, as the CHF and the HSF represent two temporally and sedimentologically distinct river systems (e.g. Hounslow and McIntosh, 2003; Morton et al., 2013; Newell, 2018a). Furthermore, multiple tributaries and bifurcations have been interpreted for these river systems (e.g. Smith and Edwards, 1991; Morton et al., 2016; Burgess et al., 2024; Gibson-Poole et al., 2025). Nomenclature which is more spatially generic but temporally rigorous is necessary to represent these source-to-sink systems. We henceforth refer to this system as a whole as the 'Sherwood River System', with the 'Sherwood-1 River System'

referring to the rivers of the CHF, and the 'Sherwood-2 River System' referring to the rivers of the HSF.

We further adopt the term Mid-Triassic Unconformity (MTU) (*sensu* Newell, 2018a) for the early Anisian unconformity below the HSF (**fig. 4**). Its former name, the Hardegsen Unconformity (e.g. Ambrose et al., 2014), is misleading, as although likely caused by the same regional tectonic event, the Franco-German Hardegsen Unconformity is distinctly older than its British equivalent (Hounslow and McIntosh, 2003). The new terminology dispels any implied time equivalency between the two.

Lithostratigraphy

Our lithostratigraphic synthesis (fig. 4) builds on the standardised nomenclature in Howard et al. (2008) and Ambrose et al. (2014). The stratigraphy in Figure. 4 is arranged by depocentre from south to north, i.e. down the depositional system. Basin-scale lithostratigraphic divisions are also depicted to aid correlation, and to better illustrate the spatio-temporal evolution of the SSG and MMG. Although the correlations of Howard et al. (2008) and Ambrose et al. (2014) terminate in the EISB and Solway Basin respectively, the SSG and lower MMG can be correlated further (e.g. Jackson et al., 1997; Mange et al., 1999; 2007; Simms, 2009) and we integrate these areas into our stratigraphic framework.

On the largest scale, the SSG is divided into four formations in accordance with Ambrose et al. (2014): the Hopwas Breccia Formation, the CHF, WSF, and HSF. The lower MMG, in accordance with Howard et al. (2008), is divided into the TSF and the SMF (**fig. 4**). The SSG overlies various Permo-Triassic units that represent the initial, post-Variscan basin fill, however the lithostratigraphy of these units has not been standardised by the BGS.

The HSF represents the second period of fluvial activity within the SSG. In the western Wessex Basin, the HSF is divided into 4 well-characterised members at outcrop: the aeolian West Down Member, and the fluvial Otterton Ledge, Chiselbury Bay and Pennington Point Members (fig. 4, Newell, 2018b). The West Down Member lies over a prominent ventifact

horizon developed at the top of the CHF: a manifestation of the MTU. In the Central Wessex Basin, the HSF is divided into five units (**fig. 4**, in this study labelled units I-V), each separated by widespread floodplain-playa deposits (McKie et al., 1997). In the Southampton 1 borehole, the HSF is divided into two units by lithology (Thomas and Holliday, 1982) and heavy mineral composition (**fig. 4**, SSG-2 and -3 in Morton et al., 2016).

In the Worcester Basin, the HSF is divided into three members, each with decreasing depositional energy (**fig. 4**, Old et al., 1991; Barclay et al., 1997; Sumbler et al., 2000). The HSF of the Worcester Graben passes gradationally upwards and northwards into the TSF, which in term grades into the SMF. The HSF is undivided in the Knowle, Needlewood, Hinkley and Stafford Basins of the Midlands, and similarly grades into the TSF and then the SMF (**fig. 4**).

The HSF is absent from the East Midlands Shelf as the Hardegsen Tectonic Event uplifted the Pennine-Charnwood Ridge, preventing sediment routing to the northeast (Warrington and Ivimey-Cook, 1992; Ambrose et al., 2014; Newell, 2018a; Newell, 2023). A ventifact horizon, marking the MTU, lies on top of the CHF in this area (Burley, 1987). The East Midlands Shelf became reconnected to the Hinkley Basin during the deposition of the MMG (fig. 4; Ambrose et al., 2014; Jones et al., 2025).

In the Cheshire Basin, the HSF is typically divided into the fluvio-aeolian Thurstaston Member, the pebbly-sandy fluvial Delamere Member and the fluvio-aeolian Frodsham Member (fig. 4; Ambrose et al., 2014). Notably, in the northwest Cheshire Basin (fig. 3), the Thurstaston Member may be part of the WSF instead of the HSF (Earp and Taylor, 1986; Hough, 2002). It is likely that these members represent large-scale, interdigitating facies associations (Thompson, 1970a; Burley, 1987; Plant et al., 1999). Above, the HSF grades into the TSF, and locally contains the aeolian Malpas Sandstone Member (fig. 4; e.g. Plant et al., 1999; Wilson, 1993; Jackson et al., 1995; Mikkelsen and Floodpage, 1997). The TSF then grades into the SMF (Plant et al., 1999). The Northwich Halite Member lies within the SMF

and forms a lithologically uniform marker unit across the basin (**fig. 4**, e.g. Evans and Holloway, 2005; Evans et al., 2011).

357

358

359

360

361

362

363

364

365

366

367

368

369

370

371

372

373

374

375

376

377

378

379

380

381

382

383

In the EISB, the MTU disappears (Jackson et al., 1995), and the HSF and WSF appear conformable (fig. 4). No accepted division of the HSF exists on a basin scale. The HSF has been variously divided into two or three members (Jackson et al., 1997). In the Morecambe Gas Field (fig. 3), the HSF is split into four members, following the tripartite stratigraphy of the HSF in the Cheshire Basin with the addition of a Waterstones Member (Bushell, 1986). However, any stratigraphic equivalency implied by the assignment of members is misleading, because these members represent large-scale, interdigitating facies associations, as previously noted for the HSF in the Cheshire Basin. The isochronous and widespread 'Century Playa' interval, (fig. 4; Thompson and Meadows, 1997; Meadows, 2006) is the only consistent, correlatable unit occurring throughout the EISB. The top of the HSF is sharp with the overlying MMG. The TSF is only present in the in the southeastern part of the EISB (Burley, 1987; Scorgie et al., 2021), with the SMF directly overlying the HSF elsewhere (fig. 4). The stratigraphic nomenclature of the MMG differs between the offshore basin centre and onshore eastern basin margin in Lancashire, but strata in these locations are directly correlatable: the Leyland Formation in the central EISB is equivalent to the Singleton and Kirkham Mudstone Members of the SMF onshore, and the Preesall, Mythrop and Rossall Halites are directly equivalent in both regions (fig. 2, 4). The Preesall Halite is also the lateral equivalent of the Northwich Halite of the Cheshire Basin (fig. 4; Jackson et al., 1995; Howard et al., 2008).

In the Peel, Kish Bank and Central Irish Sea Basins, the Ormskirk Sandstone Formation is equivalent to the HSF in the EISB (**fig. 4**, Mange et al., 1999; 2007; Floodpage et al., 2001; Merlin Energy Resources Consortium, 2020). The Leyland Formation and Preesall Halite of the MMG also correlate to their equivalents in the EISB (Chadwick et al., 2001; Merlin Energy Resources Consortium, 2020).

In the Solway Basin, the HSF is undivided (**fig. 4**, Ambrose et al., 2014). The lower part of the Stanwix Shales of the MMG is equivalent to the SMF in the EISB (Jackson et al.,

1995; Floodpage et al., 2001; **fig. 4**), with the Silloth Halite equivalent to the Preesall and Northwich Halites in the EISB and Cheshire Basin.

In the Northern Irish Larne Basin, HSF-equivalent units are absent, and instead the siltstone-rich Lagavarra Formation (**fig. 4**) is present above the MTU (e.g. Jackson et al., 1995; Simms, 2009). The Larne Halite of the SMF is likely correlative with the Preesall and Northwich Halites of the EISB and Cheshire Basin, respectively (Jackson et al., 1995).

Chronostratigraphy

The base of the HSF, i.e. the MTU and its correlative conformities (**fig. 4**), is magnetostratigraphically dated to the lower Anisian in both the Wessex Basin and the EISB (Mange et al., 1999; 2007; Hounslow and McIntosh, 2003). This boundary is thus an approximately isochronous surface, at c. 246.5 Ma (Ogg et al., 2020).

The top of the HSF, i.e. the SSG-MMG boundary, becomes progressively older to the north (fig. 4). In the western Wessex Basin, the HSF-SMF boundary is magnetostratigraphy dated to the lower Ladinian (Hounslow and Gallois, 2023), at c. 239.6 Ma (Ogg et al., 2020). In the Worcester Basin, palynological dating puts the upper part of the HSF within the Anisian or possibly the lower Ladinian, with the SMF being Ladinian in age. (fig. 4; Barclay et al., 1997). In the Midlands, the lower SMF itself is Anisian in age (fig. 4; Bridge and Hough, 2002). On the East Midlands Shelf, no widely correlatable lithostratigraphic horizon within the lower SMF exists above the Anisian-aged TSF (Howard et al., 2008). In the East Irish Sea Basin, the top of the HSF is mid-Anisian (lower Pelonsian) in age (Mange et al., 1999; 2007; Hounslow and McIntosh, 2003), at c. 244 Ma (Ogg et al., 2020, fig. 4).

Within the MMG of the Cheshire and East Irish Sea Basins, the Northwich and Preesall Halites (**fig. 4**) record marine transgressions (Greenwood and Habesch, 1991; Thompson and Meadows, 1997) and their top provides an isochronous surface of upper Anisian age (Jackson et al., 1995; Evans et al., 2011; Chedburn et al., 2022). The Anisian-Ladinian boundary (c.

241.5 Ma, Ogg et al., 2020), lies just above this marker unit (fig. 4), within the upper Byley Mudstones in the Cheshire Basin (Plant et al., 1999) and within the lower Kirkham Mudstones in the EISB (Wilson and Evans, 1990). The Silloth and Larne Halites in the Solway and Larne basins (Jackson et al., 1995; Simms, 2009) are thought to be equivalent to the Preesall and Northwich Halites, and therefore are of equivalent age (fig. 4).

410

411

412

413

414

415

416

417

418

419

420

421

422

423

424

425

426

427

428

429

430

431

432

433

434

435

436

From these chronostratigraphic constraints, a single, time-equivalent interval, defined in duration by activity of the Sherwood-2 River System, can be projected down the sediment routing system: Sequence S2. The base of S2 (fig. 4, c. 246.5 Ma, Ogg et al., 2020) is taken at the MTU between the Wessex Basin and Cheshire Basin, and its correlative conformity (the HSF-WSF boundary) in the EISB, Solway Basin, Kish Bank Basin, Peel Basin and Central Irish Sea Basin. In Northern Ireland, the base of S2 is taken as the unconformity at the base of the TSF. The top of Sequence S2 follows the Anisian-Ladinian boundary (c. 241.5 Ma, Ogg et al., 2020) as closely as possible, but is defined separately for each basin. In the Wessex Basin, the top of Sequence S2 follows the HSF-SMF boundary, which is lower Ladinian in age (Hounslow and Gallois, 2023), c. 239.6 Ma (Ogg et al., 2020). The true Anisian-Ladinian boundary is within the upper Otterton Ledge Member of the HSF the western Wessex Basin (Hounslow and Gallois, 2023), however the absence of correlation elsewhere in the Wessex Basin prevents this boundary from being used. In the Worcester Graben, the Midlands and the East Midlands Shelf, we use the TSF-SMF boundary as the top S2 sequence boundary. This stratigraphic boundary is roughly of Anisian-Ladinian age in the Worcester Graben. Although the boundary becomes substantially older in the Midlands and the East Midlands Shelf, the absence of better stratigraphic markers and the removal of the SMF by erosion means the top TSF horizon remains the best option for correlation. In the Cheshire Basin, EISB and further north, the top of S2 is taken at the top of the Northwich and Preesall Halite Members of the SMF and their stratigraphic equivalents, which are late Anisian in age (fig. 4).

In summary, Sequence S2 encompasses the HSF, the TSF, and the SMF up to and including the Preesall and Northwich Halites and their stratigraphic equivalents. Sequence S2

has a duration of approximately 5 Ma, but this may be longer in the Wessex Basin (c. 6.9 Ma), and substantially shorter in the Midlands Basins.

Palaeogeography and fairway extent

437

438

439

440

441

442

443

444

445

446

447

448

449

450

451

452

453

454

455

456

457

458

459

460

461

462

The mapped Permo-Triassic outcrop extent and sediment fairway corresponding to Sequence S2 is presented in **Figure 5**. Overall, the mapped fairway (grey colours) encompasses an area between the Wessex Basin in the south and the Central Irish Sea, Kish Bank and Peel Basins in the north. The fairway is surrounded by major upland areas, and smaller highs which separate basins. Adjacent depocentres, such as the Cardigan Bay Basin and the Plymouth Bay Basin, are also shown. Significant fault systems, and the distribution of Permian and Triassic outcrop are also depicted.

The southernmost depocentre is the Wessex Basin, which is bounded by the Central English Channel High to the south, the Start-Cotentin High to the southwest, and the Cranborne-Fordingbridge High and Mendip High in the north (fig. 5, Newell, 2018a; b). While the Wessex Basin was previously considered a basin produced largely by E-W trending normal faults (e.g. Buchanan, 1998; Butler, 1998; Hawkes et al., 1998; Underhill and Stonely, 1998; Miliorizos and Ruffell, 1998), emerging evidence suggests that Triassic extension was largely controlled by an older set of N-S extensional faults, consistent with the Triassic stress regime and structural configuration of the Wessex Basin (Newell, 2018b). North of the Mendip High lies the Worcester Graben (fig. 5), a structurally controlled depocentre controlled by the East Malvern Fault, the Inkberrow Fault and the Clopton-Clapton-Northleach Fault (Chadwick and Evans, 1995; Newell, 2018a), though the SSG also onlaps the pre-Permian basement to the west. There are four basins in the Midlands: the Knowle, Hinkley, Needlewood and Stafford basins (fig. 5). Though structurally and sedimentologically distinct from each other (e.g. Rees and Wilson, 1988; Ambrose et al., 2014), they are grouped into a single 'Midlands Basins' geological province in our source-to-sink synthesis, owing to their connectivity and small size. The Midlands Basins are joined to the Cheshire Basin in the northwest across the Market Drayton Horst, and the East Midlands Shelf to the northeast across the Pennine-Charnwood High (fig. 5). The East Midlands Shelf is a structurally simple, east-dipping ramp, and forms the western edge of the Southern Permian Basin (McKie, 2017; Newell, 2023). The Cheshire Basin is a half-graben basin primarily bounded by the Wem-Red Rock Fault in the southeast (fig. 5), and is separated from the EISB by the Llyn-Rossendale Ridge (Plant et al., 1999). The EISB contains numerous N-S faults which split the basin into sub-basins (fig. 5, Jackson et al., 1995). Beyond the EISB, there are a series of smaller, fault-controlled depocentres, including the Solway, Larne, Peel, Kish Bank, Kingscourt and Central Irish Sea basins.

Substantial upland areas likely served as sediment sources during the Triassic (e.g. Mange et al., 1999; 2007; Meadows, 2006; Tyrrell et al., 2012; Morton et al., 2013; 2016; Burgess et al., 2024). These include the Gallic Massif to the south of the Wessex Basin (fig. 5, sensu Sass et al., 2023). The Gallic Massif encompasses the modern-day Armorican Massif, the French Massif Central and the Variscan basement surrounding them, which is currently buried under the Paris Basin and English Channel. To the west, the SSG fairway is bounded by the Cornubian, Welsh and Irish Massifs, and to the east, by the Pennine High and London-Brabant Massif (fig. 5). Smaller elevated regions are also present within the sedimentary fairway: the South Staffordshire Horst and Coventry Horst in the Midlands, and the Isle of Man Massif and the Ogham Platform in the EISB (fig. 5).

Uncertainties in fairway extent

The southwesterly extent of the HSF in the Wessex Basin is largely unknown, owing to limited exploration in the area. The southernmost direct constraints are Wells 97/12-1 (Ainsworth and Riley, 2010) and 97/24-1A (**fig. 3**). The HSF likely disappears across the Start-Cotentin high (Warrington and Ivimey-Cook, 1992), and sampled seabed outcrop in this area is dominated by the MMG (Hamblin et al., 1992). The final Permo-Triassic seabed outcrop occurs approximately halfway along the Start-Cotentin Ridge (**fig. 5**) and may represent a plausible southern limit for the sediment fairway, though lithological distributions are

compounded by the truncation of Permo-Triassic units by a Cretaceous unconformity (e.g. Ruffell et al., 1995; Benabdellouahed et al., 2014; Husein et al., 2025).

Notably, there is no prior consensus on the position or extent of the connection between the Wessex Basin and Worcester Graben (Audley-Charles, 1970; Wills, 1970; Burley, 1987; Warrington and Ivimey-Cook, 1992; Newell, 2018; Burgess et al., 2024). This connection is critical for allowing the northward routing of sediment into the Worcester Graben and beyond (Tyrrell et al., 2012; Newell, 2018). The most likely point of connection between the Wessex Basin and the Worcester Graben appears to be in the area around the Shewton and Devizes wells (**fig. 3**), where sandstone facies are present beneath the MMG. This area appears to be a N-S oriented, persistent and possibly fault-controlled depression within the Mendip High. This low point, termed the Pewsey Trough (PT, **fig. 5**), had been a depocentre since the Permian (Pullan and Donato, 2022), and continued to be a deep, distinct depocentre during the MMG later in the Triassic (Newell, 2024).

North of the Midlands, Sequence S2 is only partially preserved following post-depositional erosion. The absence of basin margin deposits analogous to those in the Wessex Basin and Worcester Graben (e.g. Smith and Edwards, 1991; Barclay et al., 1997; Newell, 2018b), palaeocurrents directed across palaeohighs (e.g. Thompson et al., 1970b; Chisolm et al., 1988), outliers of SSG (Chisolm et al., 1988), and recycled Triassic detritus incorporated into younger deposits (Walsh et al., 1980; 2018) collectively indicate that the fairway extent was greater in the past, and that the current outcrop-subcrop pattern is only a reflection of where basins were deepest. The most heavily eroded area in the fairway encompasses the East Irish Sea, Peel, Kish Bank and Central Irish Sea Basins (**fig. 5**), which are interpreted to have formerly comprised a singular 'Greater Irish Sea Basin' (*sensu* Dunford et al., 2001; Meadows, 2006). However, we do not use this term as sediment routing west of the EISB remains poorly understood.

Despite clearly having a greater distribution in the past, the inferred extent of Triassic units varies between previous interpretations (Wills, 1956; 1970; Audley-Charles, 1970;

Warrington and Ivimey-Cook, 1992; Jackson et al., 1995; Dunford et al., 2001; Hounslow et al., 2006; Bourquin et al., 2011; McKie, 2017). The depositional boundaries we choose in **Figure 5** are conservative estimates based on the lines of evidence previously discussed, and the general extent of preserved Permian sedimentation, which occurred under the same extensional tectonic regime as Sequence S2. Sequence S2 is likely to have overstepped, or at the very least equalled this distribution.

Sediment isopachs

The resulting isopach maps accurately resolve the spatial and structural configuration of the sediment fairway for the first time. Deposition of all lithostratigraphic units occurs in deep, structurally-controlled basins, with sequences thinning over inter-basin palaeohighs (**fig. 6**). Data coverage is sufficient to fully resolve sediment thicknesses between the Wessex Basin and the EISB (**fig. 6a**). Absolute sediment thicknesses are only partially resolved in the Solway and Peel basins north of the Ramsay-Whitehaven Ridge, and there are insufficient data to reconstruct sediment thicknesses to the area west of the present-day EISB (**fig. 6a**). The East Midlands Shelf (**fig. 5**) was excluded from this volumetric analysis as it was not a fluvial depocentre for the HSF, and because of the absence of widespread stratigraphic markers coeval to those defining Sequence S2 (**fig. 4**, Howard et al., 2008).

The HSF in the Wessex Basin is thickest towards the west, at 320 m (**fig. 6b**), and thins gradually towards the east. The HSF also thins substantially in the south, towards the Gallic Massif. Notably, the HSF in the Wessex Basin thickens gradually towards the centre of the basin (**fig. 6b**), and shows no clear structural control apart from the oblique-slip Quantocks-Coker-Cranborne Fault System, which bounds the Cranborne-Fordingbridge High (**fig. 5, 6b, Newell, 2017b**). This again suggests that major W-E-trending extensional faults, which were active later in the Mesozoic (e.g. Buchanan, 1998; Butler, 1998; Hawkes et al., 1998; Underhill and Stonely, 1998; Miliorizos and Ruffell, 1998) were inactive in the Triassic.

In the Worcester Graben, the HSF thickens westwards towards its faulted basin margin (**fig. 6b**). Here, the HSF reaches thicknesses of 400 m, which represent the greatest thicknesses encountered in the mapped fairway. The HSF thins again in the Midlands Basins, where sediment thicknesses are low, and appears to thicken to a maximum of approximately 220m towards the centre of the area (**fig. 6b**). The HSF in the Cheshire Basin is thickest in the southeast, where thicknesses approach 210m (**fig. 6b**). Sediment thicknesses generally thin towards the west, towards the Llyn-Rossendale Ridge, and the southwestern basin margin. HSF thicknesses in the EISB are greatest at the basin centre, at 210m (**fig. 6b**), and decrease towards the basin margins.

The TSF is predominantly concentrated in the Cheshire Basin (**fig. 6c**), where thicknesses reach 200 m in the southeast. The TSF thins to the northwest towards the southeastern EISB. Here, thicknesses do not exceed 100m. To the south, the TSF is widely distributed but thin (<50 m) in the Midlands and the Worcester Graben, locally reaching 60 m thick in the hanging wall of the East Malvern Fault.

The lower SMF (below the Preesall and Northwich Halites) (**fig. 6d**) reaches up to 410 m thick in the northeastern Cheshire Basin, although it is generally 200-400 m thick elsewhere in the basin. In the ESIB, the SMF gradually thickens towards the northwest part of the basin, where the unit reaches thicknesses of 900 m (**fig. 6d**). The SMF thins towards the Ramsay-Whitehaven Ridge, and the basin margin in the west.

The Northwich Halite in the Cheshire Basin reaches a maximum thickness of 230 m (**fig. 6e**), and is thickest along a NW-SE axis through the centre of the basin, thinning out towards the margins of the Cheshire Basin. The Preesall Halite is 570m thick in the centre of the EISB (**fig. 6e**), and is thickest along a N-S axis at the basin centre. Both the extent and the thickness of the Preesall Halite is reduced over the Llyn-Rossendale Ridge, where thicknesses do not exceed 200 m.

Sediment porosity and facies

Pore space volume was removed to obtain solid rock volumes for the lithostratigraphic units in Sequence S2. For the HSF, we used porosity estimates compiled by Medici et al. (2019a) for the EISB, Cheshire, Midlands and Worcester basins (table 2). Porosity for the Wessex Basin is estimated at 18% (table 2, Bowman et al., 1993; Newell and Shariatipour, 2016). The same value of porosity is assigned to both aeolian and fluvial deposits in the HSF in each basin. For the MMG, mean values of 14.9% for the TSF and 17.8% for the SMF (Parkes et al., 2021) were applied for all basins. The Preesall and Northwich Halites are assumed to have zero porosity.

The inferred proportion of aeolian and fluvial deposits reflects the distribution of sediment at the time of deposition, and provides insight into the sedimentary processes operating within the HSF fairway. It should be noted that this figure cannot directly represent the extent of fluvial-aeolian sediment reworking, nor the ultimate provenance of the sediments. These aspects require further sedimentological and petrographic data to discern, and are further discussed in as part of the basin-by-basin synthesis of sediment routing.

For the HSF, the proportion of fluvial deposits in the EISB is 64%, and was estimated by averaging areas covered by mapped seismic facies (figs. 8 and 9 in Meadows and Beach, 1993b). The proportion of fluvial deposits in the Cheshire Basin is 71%, and was estimated from vertical facies successions from borehole logs (figs. 6 and 7 in Thompson et al., 1970a). In the Midlands and Worcester Graben, the composition of the HSF is assumed to be 100% fluvial, as no widespread aeolian facies have been observed from outcrop, core or wireline observations (Ambrose et al., 2014). In the Wessex basin, the first-order proportion of fluvial deposits is estimated at 90% and is consistent in both the western and central areas (McKie et al., 1997; Newell, 2018b).

Sediment volumes

Solid rock sediment volumes (with porosity removed) are presented for the HSF, TSF and lower SMF for the first time in **Figure 7**, with a full breakdown available in **Supplementary Material 3**. In total, Sequence S2 encompasses 15,600 km³ of rock volume. Of this, 5,590 km³ (36%) is represented by the HSF of the SSG. The remaining 10,000 km³ (64%) is represented by the MMG. Within the MMG, 613 km³ is in the TSF, 6190 km³ in the lower SMF, and 3210 km³ in the Preesall and Northwich Halites; these lithostratigraphic units comprise 4%, 40% and 20% of the total sediment volume of Sequence S2, respectively.

By volume, the EISB is the largest basin, with a total sediment volume of 9750 km³, representing 62% of the total volume of Sequence S2 (fig. 7). However, the HSF only comprises 1820 km³ (19%) of the EISB's sediment volume, and only 1160 km³ (12%) is composed of fluvial deposits in the HSF. The Cheshire Basin is the second largest depocentre, with a total sediment volume of 2500 km³. The HSF comprises 533 km³ (21%) of the Cheshire basin's total volume, of which 379 km³ (15%) is fluvial deposits. The Wessex Basin is third largest depocentre, with a total sediment volume of 1870 km³. Sequence S2 is only composed of the HSF here, with 1690 km³ of fluvial deposit volume. The Worcester Graben has a total sediment volume of 1090 km³. Sediment volumes here are dominated by the entirely fluvial HSF, at 1030 km³ (95%). The remainder of this volume (54.5 km³, 5%) comprises the TSF. The Midlands Basins are collectively the smallest depocentre, with a total sediment volume of 386 km³. Again, this volume is dominated by the entirely fluvial HSF, at 335 km³ (87%), with 51.7 km³ (13%) being the TSF. Overall, the largest volume of HSF occurs in the Wessex Basin, followed by the EISB, the Worcester Graben, the Cheshire Basin, and then the Midlands basins (fig. 7).

When sediment volumes are integrated with the well-constrained chronostratigraphy in the EISB and Wessex Basin (**fig. 4**), solid rock sediment accumulation rates can be calculated. In the EISB, Sequence S2 has a total duration of 5 Ma: 2.5 Ma for the HSF, and 2.5 Ma the lower MMG (the TSF, SMF and Preesall Halite). In the Wessex Basin, Sequence S2 has a duration of 6.9 Ma. For the EISB, sediment accumulation rates are 726 km³/Ma in

the HSF, and then 3170 km³/Ma in the lower MMG: a greater than fourfold temporal increase. The overall accumulation rate across Sequence S2 in the EISB is 1950 km³/Ma. In the Wessex Basin, sediment accumulation rate within Sequence S2 is 271 km³/Ma.

Errors and uncertainties in sediment volume

Uncertainties in the original fairway extent cause uncertainties in mapped and calculated sediment volumes. The greatest uncertainty in fairway extent occurs in the southwestern part of the Wessex Basin, where as previously discussed, there are very few constraints on the thickness or distribution of the HSF (fig. 3). North of the Midlands (fig. 6a), uncertainties in fairway extent are caused by post-depositional erosion. This uncertainty is reduced by the fact that basin centres are fully preserved and well-constrained, with only the basin margins being eroded, where Sequence S2 is thinnest. Furthermore, as the boundaries of palaeohighs (where sediment thickness is zero) are drawn from conservative estimates of fairway extent, the resulting isopach maps and sediment volumes are also conservative estimates.

Uncertainties in defining the upper boundary of Sequence S2 in the sediment fairway are potentially high owing to sparse chronostratigraphic constraints. The volume of the HSF in the Wessex Basin is likely overestimated, based on magnetostratigraphic constraints in the Devon section of the Wessex Basin (fig. 3, 4). However, the absence of basin-scale stratigraphic correlations prevents a full quantification of this uncertainty. Current stratigraphic data suggest that volumes in the Midlands Basins may be generally underestimated compared to the idealised Anisian-Ladinian boundary (c. 241.5 Ma, Ogg et al., 2020) for Sequence S2, owing to the exclusion of the SMF in these basins. The volume of SMF excluded here is likely low, owing to the small size of the Midlands depocentres (fig. 7).

Within Sequence S2, uncertainties in the definition of lithostratigraphic boundaries are low. The stratigraphic distinction between the HSF, SMF and Preesall and Northwich Halites,

are well resolved by lithology and wireline log response, owing to their distinctive lithological characteristics (e.g. Meadows, 2006; Ambrose et al., 2014 Newell, 2018; Chedburn et al., 2022). More uncertainty occurs in areas where the TSF is gradational between the HSF and the SMF. However, the impact of this uncertainty at the fairway scale is small, as the TSF is the volumetrically smallest of the four studied units (**Fig. 7**).

Uncertainty in rock porosity is generally low in the SSG, as porosity is well-characterised from a large dataset compiled from core plug measurements from across the sediment fairway (**Table 2**, Bowman et al., 1993; Newell and Shariatipour, 2016; Medici et al., 2019a). Uncertainties in the MMG are higher, as far fewer measurements of porosity are available (Parkes et al., 2021). However, owing to the limited range of porosities in mudstones (<20%, AlNajdi and Worden, 2023), the impact of porosity on sediment volume is limited compared to the other uncertainties discussed.

The partitioning between fluvial and aeolian deposits in the HSF, particularly in the Cheshire Basin and EISB, represents a further uncertainty. Though there is good spatial coverage to adequately characterise first-order facies distributions, methods to recognise and define aeolian or fluvial deposits differ within each basin (Thompson, 1970a; Meadows and Beach, 1993b). There is also insufficient information available to characterise the mixed fluvial-aeolian deposits, beyond the assumption that they are 50% fluvial and 50% aeolian. Ultimately, the fluvial and aeolian deposit volumes represents a first-order estimation of the facies distribution within the respective basins.

Bulk sandstone mineralogy in the HSF

Bulk sandstone mineralogy in the HSF is presented in **table 3**, and is separated by study, point counting method and depocentre. Data counted using the Indiana point counting method encompass Burley (1987), Scorgie et al. (2021), and Meadows (pers. comm.). Those using the Gazzi-Dickinson method encompass Knox et al., (1984), Svendsen and Hartley

(2001), and De Sainz Simpson (2022). Data from Ali et al. (1982), and Chisholm et al. (1988), which were both collected from the Midlands Basins, could not be unambiguously classified into either point counting system and are retained in a separate category (**table 3**).

The geographic distribution of bulk sandstone mineralogical data in the sediment fairway is presented in **fig. 8a**, and bulk mineralogical variations of the HSF within each basin is presented as QFL plots in **fig. 8b** (see **Supplementary Material 4** for full dataset).

By the Gazzi-Dickinson method of point counting, quartz and feldspar are the dominant mineralogical components in the HSF, though proportions change substantially between basins. In the Wessex Basin, bulk sandstone mineralogy appears similar in both the eastern and western basin areas, with a quartz content of 50-70%, a feldspar content of 20-50% and a lithic content of 0-20% (fig. 8b; Knox et al., 1984; Hartley and Svendsen, 2001). Although there is no quantified petrographic data for the central part of the Wessex Basin (fig. 8a), its bulk mineralogy appears comparable to the eastern and western Wessex Basin (Bath et al., 1987). To the north, the HSF appears to have a similar bulk mineralogy in both the Cheshire Basin and EISB, with a quartz content of 80-95%, a feldspar content of 0-15%, and a lithic content of 0-10% (fig. 8b, De Sainz Simpson, 2022). Furthermore, fluvial and aeolian facies in the Cheshire Basin and EISB appear to have similar bulk mineralogy.

By the Indiana method of point counting, resultant proportions of quartz, feldspar and lithic fragments are more variable, though again, mineralogical proportions vary between basins. In the Wessex Basin, the HSF largely has a quartz content is of 40-70%, a feldspar content of 15-50%, and lithic content of 10-50% (**fig. 8a**, Burley et al., 1987). In the Cheshire Basin and EISB, bulk sandstone compositions are again similar, with a quartz content of 50-90%, a feldspar content of 0-25%, and a lithic content of 5-40% (**fig. 8b**; Burley, 1987; Scorgie et al., 2021; Meadows, pers. comm). In the Cheshire Basin, there appears to be a difference in bulk mineralogy between fluvial and aeolian facies, with aeolian sandstones (n = 4) being more quartz-rich than fluvial sandstones (n = 58). In the EISB, fluvial and aeolian facies appear to have a similar bulk mineralogy.

The point counting method used by Ali (1982) and Chisholm et al. (1988) is undetermined owing to the limited data present (2 localities, n = 6). Here, the quartz content of HSF is 80-90%, the feldspar content is 5-15%, and the lithic content is 2-10% (**fig. 8b**).

Overall, there is a notable difference in bulk sandstone mineralogy between the Wessex Basin in the southern part of the sediment fairway, and the Midlands, Cheshire Basin and EISB to the north. Although an absence of data in the Worcester Graben and the Midlands basins prevents a full appraisal of bulk sandstone mineralogy, sediments are clearly more feldspathic in the southern part of the fairway than the north for both point counting methods (fig. 8b). Furthermore, throughout the northern fairway, the majority of lithic fragments are igneous and metamorphic in nature (as defined by the Indiana method, Supplementary Material 4), and are composed of quartz and feldspar grains (by the Gazzi-Dickinson method) (fig. 8b). The HSF in the Wessex Basin contains the highest number of non-quartz and non-feldspar lithic fragments (as defined by the Gazzi-Dickinson method, fig. 8b).

Diagenesis and its impact on bulk sandstone mineralogy

Diagenetic alteration of unstable detrital grains also contributes to uncertainties in reconstructing original bulk sandstone mineralogy. Lithic fragments and feldspars are ubiquitously altered in the HSF across all basins, evidenced by grain dissolution textures, skeletal grains, and the presence of authigenic clays and feldspars (e.g. Ali and Turner, 1982; Burley, 1984; Knox et al., 1984; Bushell, 1986; Strong and Milodowski, 1987; Greenwood and Habesch, 1993; Plant et al., 1999; Scorgie et al., 2021). Grain dissolution porosity is measured at 7% in Devon in the western Wessex Basin, 8% in the Marchwood 1 borehole in the eastern Wessex Basin, and up to 7% in the EISB margin (Burley, 1984).

On the fairway scale, the maximum burial depth for the HSF can be used to approximate the maximum effects of diagenesis in each basin. The burial histories for each basin (fig. 9) are derived from apatite fission track analysis and vitrinite reflectance (Carter et

al., 1995; Mikkelsen and Floodpage, 1997; Bray et al., 1998; Gent, 2006; Pharaoh et al., 2018). Selected wells are located away from basin margins, and so likely represent typical burial depths for each respective basin. The maximum burial depth for the HSF at the Wytch Farm oilfield in the Wessex Basin is 3.5 km (Bray et al., 1998). The SSG in the Midlands Basins reached a palaeotemperature of 75 ± 10 °C between 150 and 70 Ma (Carter et al., 1995). Assuming a geothermal gradient of 30 °C/km, this implies a maximum burial depth of 2.5 ± 0.3 km (fig. 9b). The HSF in the Knutsford 1 well in the Cheshire Basin reached a maximum burial depth of 2.9 km (fig. 9b, Mikkelsen and Floodpage, 1997), and for well 110/7b-6 in the EISB, 1.8 km (fig. 9b, Gent, 2006; Pharaoh et al., 2018). This implies the HSF across Great Britain reached comparable maximum burial depths (c. 3km), except in the EISB, which was buried to shallower depths (c. 2km). This in turn suggests that the maximum impact of diagenesis is relatively similar in all basins except for the ESIB, which may have experienced less extreme diagenetic alteration.

These figures provide a general indication that HSF sandstones were originally more lithic- and feldspar-rich, with a modest amount (<10% of the total rock volume) of lithics and feldspars being removed during burial diagenesis. Data points in **Figure 8b** cannot be translated uniformly to remove diagenetic effects, as burial depths and diagenetic histories differ for data collected at basin margins and palaeohighs, compared to deeper basin centres (Green et al., 1995; Bray et al., 1998; Scorgie et al., 2021). However, the spread of bulk sandstone detrital mineralogy both within basins and between basins (**fig. 8b**) is substantially greater than any compositional variations expected from diagenesis. This in turn indicates that spatial variations in bulk sandstone composition in the HSF between basins is a primarily depositional signal, and so can be used to interpret sediment routing within the fairway.

Sediment routing in the HSF fairway

Our basin-by-basin source-to-sink synthesis overall supports the idea of the Sherwood-2 River System as a continuous, south to north running fluvial system during deposition of Sequence S2 (fig. 10). We also resolve the presence of secondary sediment inputs and fluvial-aeolian interactions, and provide insight into sediment routing beyond the EISB and across the transition between the SSG and MMG (i.e. the distal segments of the Sherwood-2 River System). This section serves as a summary of sediment routing, whereas a more detailed overview of sediment routing in the Wessex, Cheshire and East Irish Sea Basins, as well as the SSG-MMG transition, is presented in **Supplementary Material 5** to honour the breadth and depth of published information available.

Sediment routing within the HSF

In the Wessex Basin, quantitative provenance analysis indicates the Sherwood-2 River System operated as a series of at least three north-flowing tributaries (**fig. 10a,** Morton et al., 2016). The HSF is dominated by material with a Variscan-Cadomian provenance, sourced from the basement units of the Gallic Massif (Tyrrell et al., 2012; Morton et al., 2013; 2016). This is supplemented by material sourced from the granites of the Cornubian Massif (Smith and Edwards, 1991) and recycled Devonian sediment from the London-Brabant Massif (Morton et al., 2016). All tributaries likely coalesced south of the Pewsey Trough and flowed nothwards as a single trunk river into the Worcester Graben (**fig. 10a**).

In the Worcester Graben, the main axis of sediment routing was to the north (**fig. 10a**, Old et al., 1991). Breccias and conglomerates are found in several places along the length of the East Malvern Fault, implying local sediment inputs from the Welsh Massif (Barclay et al., 1997). However, there are no contemporary studies of sediment provenance or petrography in the Worcester Graben and so the details of sediment routing here are largely unknown.

In the Midlands Basins, recorded palaeocurrent azimuths suggest the primary axis of sediment routing was northwards (**fig. 10a,** Old et al., 1987; 1991, Chisolm et al., 1988). Multiple sediment inputs from the Welsh and London-Brabant Massifs are proposed by

Audley-Charles (1970), based on observed clast compositions in the HSF (**fig. 10a**). The pronounced difference in HSF bulk sandstone composition between the Wessex Basin and the Midlands basins (**fig. 8b**) suggests that substantial dilution of Variscan-derived material by sediments from other source areas had already occurred before the Sherwood-2 River System reached the Midlands Basins (Plant et al., 1999; Morton et al., 2013). However, bulk sandstone mineralogical data for the Midlands Basins is limited (**fig. 8b**), and thus the mineralogical diversity of the HSF here may not be fully captured. The CHF in the Midlands appears to have a substantial lithic component (Indiana method, Burley, 1986) which may also be present in the HSF.

During much of Sequence S2, an emergent Pennine-Charnwood Ridge disconnected the Sherwood-2 River System from the East Midlands Shelf, evidenced by the presence of ventifacts at the top of the CHF in this area (Burley, 1987; Newell, 2023). Accordingly, the East Midlands Shelf was devoid of large-scale fluvial activity, and was instead a low-energy coastal plain where the MMG was deposited (Jones et al., 2025). Reconnection between the Midlands and the East Midlands Shelf occurred during the latter stages of Sequence B2 during deposition of the TSF (fig. 10a).

In the Cheshire Basin, palaeocurrents suggest the main axis of fluvial transport was towards the northwest (**fig. 10a,** Thompson, 1970b; Plant et al., 1999; Mountney and Thompson, 2002; De Sainz Simpson, 2022; Cosgrove et al., 2025). This was accompanied by input of fluvial sand from the Welsh Massif (Plant et al., 1999) (**fig. 8b**). A further component of aeolian activity is associated with the fluvial system. Palaeowinds originated from the east, and aeolian sediment was sourced from the Pennine High (**fig. 10a**, Thompson, 1970b; Rees and Wilson, 1998; Mountney and Thompson, 2002; De Sainz Simpson, 2022; Cosgrove et al., 2025). The proportion of fluvial and aeolian deposits is highly variable both spatially and temporally (e.g. Burley, 1987; Cosgrove et al., 2025), and their distribution likely had underlying climate and subsidence controls, which in turn controlled sediment flux, accommodation generation, and water table level (Newell, 2018; Cosgrove et al., 2025). In

spite of this variability, a throughgoing fluvial system was maintained, as widespread and perennial fluvial activity occurred downsystem throughout the EISB (Meadows and Beach, 1993a; b; Meadows, 2006).

805

806

807

808

809

810

811

812

813

814

815

816

817

818

819

820

821

822

823

824

825

826

827

828

829

830

831

In the EISB, the Sherwood-2 River System entered the basin in the south, and then turned west (Cowan, 1993; Herries and Cowan, 1997; Plant et al., 1999; Dunford et al., 2001; Meadows, 2006; Marsh et al., 2022). Here, Mange et al. (1999, 2007) also identifies a sediment input from the Welsh Massif (fig. 10a), though this signal may have propagated from the Cheshire Basin. There was also an aeolian sediment source from the Pennine High to the east (fig. 10a, Meadows and Beach, 1993a; Jones and Ambrose, 1994; Meadows, 2006; Scorgie et al., 2021; Marsh et al., 2022). There was likely considerable aeolian reworking of fluvial sediments in the EISB prior to deposition: monocrystalline feldspars within both fluvial and aeolian facies have a provenance signal suggesting a Gallic Massif source (Tyrrell et al., 2012). There is no systematic variation in mineralogy between facies (fig. 8b) suggesting that these feldspars were also well-mixed in the basin. The provenance of the lithic fragments, which are composed primarily of quartz and feldspar and are also present in the Cheshire Basin (fig. 8b), is currently unknown. Basin margins are 100% aeolian (Jones and Ambrose, 1994; Medici et al., 2019a), whereas major fluvial activity is maintained in the basin centre, with aeolian facies only comprising 5-10% of the rock volume (Cowan, 1993). In more detail, spatial partitioning of fluvial and aeolian deposits in the basin may have followed structurally controlled highs and lows (Meadows and Beach, 1993b).

After the EISB, the Sherwood-2 River System flowed further west to the Kish Bank, Peel, Central Irish Sea basins. These basins formerly formed a contiguous depocentre with the EISB (**fig. 10a,** Dunford et al., 2001; Meadows, 2006; Marsh et al., 2022). The sedimentology of the HSF in these basins is poorly characterised relative to the rest of the HSF fairway, a problem exacerbated by the severe degree of post-Triassic erosion in the area. All basins contain a mix of fluvial and aeolian sandstone facies (Newman, 1991; Naylor et al., 1993; Dunford et al., 2001; Floodpage et al., 2001).

The Irish Sea area was unlikely to be the ultimate terminus of the Sherwood-2 River System, as there is no indication of an endorheic terminal splay system here (e.g. McKie, 2011; 2014, Gibson-Poole et al., 2025). Topographic barriers and an absence of fluvial facies indicate the Sherwood-2 River System did not flow north towards the Solway and North Channel basins (**fig. 10a**, Marsh et al., 2022) or south into the Celtic Sea Trough (**fig. 10a**, Dunford et al., 2001). It is most likely that the Sherwood-2 River System therefore flowed west the via the Kingscourt Basin, possibly draining externally towards the shallow marine Porcupine Basin, west of Ireland (Croker and Shannon, 1987).

Sediment routing across the SSG-MMG transition

The onset of MMG deposition is diachronous (**fig. 4**), and coincides with the Muschelkalk marine transgression, which was accompanied by climatic aridification (Greenwood and Habesch, 1991; Thompson and Meadows, 1997; McKie, 2014; Newell, 2018). This transgression likely originated from the marine domain west of Ireland (Croker and Shannon, 1987), and manifests as a successive backstepping of fluvial activity and an ingress of halite lake and playa facies, initially into the EISB, but then into the Cheshire Basin, Midlands basins and Worcester Graben (**fig. 10b**).

In the EISB, there is a sharp transition from the aeolian and sabkha deposits of the HSF into the playa lake deposits of the SMF (**fig. 4**, Meadows and Beach, 1993a; Thompson and Meadows, 1997; Meadows, 2006). In the Cheshire Basin, the aeolian-dominated upper HSF transitions into the playa margin deposits of the TSF (**fig. 4**; **6c**; Mikkelsen and Floodpage, 1989; Burley, 1987; Scorgie et al., 2021; De Sainz Simpson, 2022), which are mineralogically distinct from the underlying HSF (Scorgie et al., 2021). In the Midlands Basins and Worcester Graben, the fluvial deposits of the HSF transition into playa margin, fluvial and estuarine deposits of the TSF (e.g. Warrington, 1970a; b; Charsley, 1982; Old et al., 1991; Barclay et al., 1997; Warrington and Pollard, 2021; Jones et al., 2025), although these latter successions are

thin and impersistent (**fig. 6c**). The Worcester Graben represents the southern limit of the brackish and/or marginal marine deposits of the TSF (Fig. 4). In the Wessex Basin, the uppermost HSF is fluvial in the west (Newell, 2017b), and composed of ephemeral lacustrine and sandflat deposits in the basin centre (McKie et al., 1997). Both areas then transition into the arid playa lake mudstones of the SMF (**fig. 4**).

Although sand-grade sedimentation ceased during the deposition of the MMG, sediment fluxes were sufficient to fill basins approximately to base level, with the fairway seeing brief, but regular marine transgressions. In the EISB, sediment accumulation rates appear to be substantially greater in the MMG than the SSG. Indeed, rift activity is known to be variable during the Triassic (Newell, 2017a), and this general increase in accommodation may have also contributed to the southwards retreat of sand-grade deposition (e.g. Paola and Martin, 2012; Reynolds, 2024). Without better chronostratigraphic constraints and decompaction, the impact of active faulting on sedimentation during this time interval remains uncertain.

The assemblage of evaporitic playa lake, playa margin, and intercalated fluvial-aeolian deposits in the SMF, TSF and HSF (**fig. 4**) corresponds well to a terminal splay depositional model (e.g. Lang et al., 2004; McKie, 2011, 2014), in which incoming fluvial systems are dispersed at a playa margin. Fluvial activity becomes increasingly ephemeral and unconfined, and declines rapidly towards the basin-centre playa lake (**fig. 10b**). The SSG-MMG transition therefore represents the southward retreat of the Sherwood-2 River System. The absence of evidence of fluvial activity in the upper HSF and TSF in the EISB and Cheshire Basin may be due to preservational bias, as inactive fluvial deposits were rapidly reworked and incorporated into playa margin and aeolian deposits (Lang et al., 2004; McKie, 2011).

In the EISB and Cheshire Basin, the large volumes of SMF observed (figs. 4, 6d, e) were deposited in ephemeral lacustrine and dry mudflat settings (Arthurton, 1980; Wilson, 1990; 1993). The provenance of the MMG has not been directly addressed in this part of the UK, though ephemeral lacustrine deposits were likely sourced from flash floods, of which the

Sherwood-2 River System would have been a contributor. Dry mudflat deposits require fine sediments with an aeolian source. In modern arid settings, fine sediments are highly mobile, and can be transported for hundreds of kilometres by dust storms (Jefferson et al., 1990; Brookfield, 2008; McKie, 2011; Mao et al., 2021; Marx et al., 2022). While the nature of lacustrine-aeolian reworking, as well as preservational biases within playa settings, require further study (McKie, 2011), it is probable that not all the mudstone within the SMF has an origin from the Sherwood-2 River System. West-blowing Triassic palaeowinds may have served to rework sediment both into, within and out of these basins (**fig. 10b**).

Source areas and regional correlation of the Sherwood-2 River System

Palaeo-lithological domains

Pre-Triassic bedrock located in upland areas (fig. 11) represents the ultimate source of sediment for the Sherwood-2 River System. The pre-Triassic surface of northwestern Europe is lithologically diverse, and encompasses an area from the core of the Variscan Orogeny in the south (Baptiste, 2016; Martínez Catalán et al., 2021) to the Palaeozoic sedimentary cover of cratonic Avalonia in the north (Butler, 2018). There is considerable lithological uncertainty where the pre-Triassic surface is buried under more recent sedimentary cover, such as in the Paris and Weald basins (Baptiste, 2016; Butler, 2018). Uncertainties are exacerbated by the fact that the Triassic distribution of basement lithologies is unknown. However, it is well-documented that key Variscan basement units had already exhumed by the end of the Carboniferous (c. 300 Ma) and were supplying sediment to the British Isles (e.g. Hallsworth et al., 2000; Jones et al., 2011; Morton et al., 2021; 2024).

We base our sediment routing interpretations on characterisation of source lithologies by their first-order composition and their tectonic domain. This results in a division into the internal Variscan metamorphic units and dominantly sedimentary domains. Where possible, we focus on the distribution of granitoids and gneisses, which provide provenance-sensitive feldspars, zircons and other heavy minerals to their respective fluvial catchments (Paul et al., 2008; Sanchez Martínez et al., 2012; Tyrrell et al., 2012; Morton et al., 2013; 2016; Augustsson et al., 2018; Sass et al., 2023). Additional constraints on sediment routing, including inferences made from known constraints on palaeotopography, can be found in **Supplementary Material 5**.

Internal Variscan metamorphic units

The internal Variscan metamorphic units comprise a complex sequence of tectonic domains, which collectively form the core of the Variscan Orogen in northwest Europe. The Mid-Variscan Allochthon forms much of the basement in central France (**fig. 11**). Variscanaged granitoids, gneisses and migmatites are found throughout this unit, and are presently the most common group of rocks (Baptiste, 2016; Catalán et al., 2021). The North and Central Armorican tectonic domains to the north are primarily composed of metasediments and, respectively, Cadomian-aged granitoids and gneisses and Varican granites (**fig. 11**, Baptiste, 2016). The northernmost tectonic domain is the Léon-Normannian-Saxothuringian Domain, which lies mostly at subcrop and under the English Channel in the study area, and is poorly characterised (Shail and Leveridge, 2006). However, in north Brittany, this domain contains Variscan granitoids (Catalán et al., 2021). In the east, this domain also contains Cadomian granitoids or gneisses, and the Variscan Barfleur Granite (Baptiste, 2016; Donato et al., 2023).

The Gallic Massif is entirely composed of the internal Variscan metamorphic units. (**fig. 10a, 11**). In the Wessex Basin, the delivery of Variscan-aged feldspars to the HSF necessitates a sediment source in the Central Armorican Zone and Mid-Variscan Allochthon, where the closest Variscan granitoids are concentrated. This yields approximately 300 km of non-preserved drainage for the Sherwood-2 River System over the Gallic Massif (**fig. 11**). In

the central and eastern Wessex Basin, observed Variscan ages (Morton et al., 2016) are likely derived from the Barfleur Granite in northern France, owing to its proximity to the sediment fairway (fig. 11). In southern Brittany, the Biscay Rift likely directed fluvial systems south towards the Iberian Peninsula (fig. 11, Péron et al., 2005; Bourquin et al., 2011; Sanchez Martínez et al., 2012). The remaining part of the Gallic Massif is inferred to have supplied the Franco-German Buntsandstein (fig. 11). This configuration allows for Cadomian and Variscan source signals to be supplied to this latter sediment routing system (Paul et al., 2008; Augustsson et al., 2018; Sass et al., 2023).

Dominantly sedimentary domains

Two basement tectonic domains are predominantly composed of sedimentary rocks: the Rhenohercynian Zone (RHZ), which represents the Variscan fold-and-thrust belt, and Cratonic Avalonia, which has experienced mild to no Variscan deformation (fig. 11). Both domains are both composed of synorogenic Variscan clastic sediments, as well as older carbonates and clastics predating the Variscan Orogeny (e.g. Butler, 2018). The RHZ additionally hosts Variscan granites of the Cornubian Batholith, with an associated contact metamorphic aureole (fig. 11, Searle et al., 2024). The geology beneath the Variscan unconformity has been illustrated in detail by Butler (2018). These two domains were likely equally as lithologically diverse during the Triassic as they are currently, though their internal distribution of lithologies would have favoured the younger and stratigraphically higher Carboniferous rocks which have since been removed by erosion.

The catchment for the Sherwood-2 River System likely extended into the Cornubian Batholith in the RHZ, around 30 km west of the Wessex Basin (**fig. 4**) (Smith and Edwards, 1991; Morton et al., 2013). On the eastern side of the Wessex Basin, the London-Brabant Massif lies in both the RHZ and Cratonic Avalonia, and has potential to provide a sizeable drainage area into the S2 fairway. However, the extent of the drainage which supplied recycled Devonian clastics from the London-Brabant Massif (Morton et al., 2016) is unclear owing to

the large areal extent of this source, and the abundant subcrop of this lithology beneath the Variscan unconformity (Butler et al., 2018). The Welsh Massif also has potential to supply a sizeable drainage area for the S2 fairway (**fig. 10a**), and HSF sandstones in the EISB appear to have been derived from North Wales (Mange et al., 1999), though the overall extent of this catchment remains unclear. The Pennine High separates the mudstone-dominated East Midlands Shelf from the sandstone-dominated EISB, and was a well-documented sediment source for the latter (Meadows and Beach, 1993a; Meadows, 2006; Scorgie et al., 2021; Marsh et al., 2022). The Pennine High was likely small in extent and/or elevation, implied by the lack of fluvial activity on the East Midlands Shelf (Howard et al., 2009; Jones et al., 2025).

963

964

965

966

967

968

969

970

971

972

973

974

975

976

977

978

979

980

981

982

983

984

985

986

987

988

989

Sediment routing over the London-Brabant and Welsh massifs remains poorly known owing to the absence of sediment routing constraints in the Midlands and Worcester Graben, as previously discussed in the context of mineralogy and basin-by-basin sediment routing. After the Gallic Massif, the London-Brabant and Welsh massifs constitute the second and third largest potential catchment sources by areal extent (fig. 11). Given that topography declined and aridity generally increased northwards of the Variscan mountains (Péron et al., 2005; McKie, 2014), comparatively large sediment fluxes from these uplands may have entered the Sherwood-2 River System in the Worcester Graben or in the Midlands basins. This sediment was likely lithic-rich and felspar-poor, containing lithoclasts of metasediments, volcanic rocks, carbonates and chert, and reflecting the mineralogy of recycled Devonian and Carboniferous sandstones (Knox et al., 1984; Glover and Powell, 1995; Bridge et al., 1998; Jones et al., 2011). Although bulk sandstone mineralogy clearly changes between the Wessex Basin and the Midlands, there is no evidence for lithic fragments of this nature being present in the northern part of the sediment fairway. In this area, lithic fragments are instead composed of quartz and feldspar (fig. 8b). Hence, the changes in bulk mineralogy observed (fig. 8b) require further study. These mineralogical changes may not only be a product of interactions between different source areas, but also the breakdown of recycled lithic fragments and feldspar during sediment transport and then diagenesis.

Discussion and Conclusions

Overall, the stratigraphic architecture of Sequence S2 is controlled by a gradual increase in base level and an inferred increase in aridity during the latter part of the Anisian (e.g. Newell, 2017a; McKie, 2017). The Sherwood-2 River System was likely initially externally draining, but continued aridification meant that for the majority of Sequence S2, the fluvial system largely ended in terminal splay systems, discharging into a network of playa lakes with intermittent marine influence. Semiarid fluvial and aeolian deposits of the HSF were gradually replaced by mudstone-dominated playa and halite lake facies within the MMG (fig. 4, 10a, b).

Within Sequence S2, the EISB is the largest sediment sink within the mapped fairway, representing 62% of the total sediment volume deposited during this interval (**fig. 7**). Although sand-grade sedimentation ceased during the deposition of the MMG, sediment fluxes were sufficient to fill basins close to base level. As previously discussed, sediment accumulation rates appear to have been temporally variable, and likely structurally controlled (Newell, 2017a), although a paucity of chronostratigraphic constraints within Sequence S2 itself means that our understanding of this control on sediment deposition remains limited.

North-flowing paleocurrents in the HSF (**fig. 10a**) and the widespread distribution of Variscan-Cadomian material throughout the sediment fairway (e.g. Mange et al., 1999; Plant et al., 1999; Tyrrell et al., 2012; Morton et al., 2016), suggest that the Sherwood-2 River System was one, continuous river network. On the other hand, substantial changes in bulk sandstone mineralogy (**fig. 8b**) and differences in heavy mineral indices between basins (Plant et al., 1999; Morton et al., 2013) suggest sediment composition changes substantially within the fairway. The HSF in the Wessex Basin is dominated by feldspathic sediments supplied from the Gallic Massif, which by area and elevation was the largest catchment feeding the Sherwood-2 River System (**fig. 11**). The bulk mineralogy of the HSF in the Wessex Basin contrasts with that of the Midlands basins, Cheshire Basin and EISB, where sediments are

substantially more quartz-rich (**fig. 8b**). This petrographic change implies sediment composition was substantially modified in the Worcester Graben or the Midlands basins (**fig. 8a**), although variations in bulk sandstone mineralogy are likely not only the result of additional tributary input, but also the breakdown of lithic fragments and feldspars during transport and diagenesis. In the Cheshire Basin and the EISB, fluvial and aeolian inputs of sediment are well-documented, and these basins served as considerable domains for fluvial-aeolian interactions. Aeolian processes may have continued to be a substantial conveyor of sediment during the deposition of the MMG, and served to both input and export sediment from the fairway.

Evidence for additional fluvial inputs into the Sherwood-2 can be further observed when the fluvial systems of the SSG are compared to modern analogues in the Kati Thanda–Lake Eyre Basin (Brookfield, 2008; McKie 2014; Morón et al., 2014; English et al. 2024). Under semiarid climates and with no secondary inputs, these modern river systems experience high transmission losses of around 80% over approximately 200 km (Costelloe et al., 2000), and are mostly ephemeral. Despite a comparable climatic setting, the Sherwood-2 River System was perennial in both its proximal and distal reaches over a length scale of 500km (Meadows and Beach, 1993; McKie et al., 1997; Meadows, 2006). As such, secondary fluvial inputs may have been important in maintaining a consistently perennial fluvial system, consistent with the substantial sediment inputs into the Sherwood-2 north of the Wessex Basin expressed in bulk sandstone mineralogy. Similarly, the decline of these proximal sources of sand during the onset of aridification may have contributed in generating the SSG-MMG transition, which occurred in the northern part of the fairway despite a sustained semiarid climate in the Wessex Basin (Newell, 2017b) and steady supply of fluvial sediment from the Gallic Massif recorded by the time-equivalent HSF there (Tyrrell et al., 2012; Morton et al., 2016).

In conclusion, through the creation of a new chrono- and lithostratigraphic framework, and an up-to-date paleogeographic framework for the mid-Triassic of the British Isles, we are able to resolve the spatial and temporal dynamics of the HSF, TSF and lower SMF, and

construct a source-to-sink depositional model linking the three units. Although the Sherwood-2 River System was unambiguously a single, major fluvial system flowing across the British Isles, substantial changes in bulk sandstone mineralogy, supported by a basin-by-basin synthesis of sediment routing, reveals that there were likely multiple, substantial sediment inputs north of the Wessex Basin. The temporal evolution of the Sherwood-2 river system was dominated by a southwards retreat of fluvial deposits of the HSF, which were replaced by playa-lacustrine deposition of the TSF and SMF. This change is typically attributed to a regional increase in base level and aridity. However, a greater than fourfold increase in sediment accumulation rate is observed in the EISB, the largest depocentre in the sediment fairway. As such, tectonics likely serves as a previously unrecognised control on stratigraphic architecture during this time interval.

Acknowledgements

We thank the UK Onshore Geophysical Library, the British Geological Survey, the Bureau de Recherches Géologiques et Minières, EDINA, and the North Sea Transition Authority National Data Repository for providing data used for analysis and visualisation in this study. We thank Neil Meadows and Stuart Burley for insightful discussions about the Sherwood Sandstone Group, and for supplying petrographic data.

Author contributions

XY: Conceptualization (lead), Data curation (lead), Formal analysis (lead), Investigation (lead), Methodology (lead), Visualization (lead), Writing – original draft (lead), Writing – review & editing (equal); GJH: Funding acquisition (lead), Methodology (supporting), Supervision (equal), Visualization (supporting), Writing – review & editing (equal); ACW: Funding

1067	acquisition (supporting), Methodology (supporting), Supervision (equal), Visualization
1068	(supporting), Writing – review & editing (equal).
1069	
1070	Funding
1071	This work was funded by the Natural Environment Research Council (Grant NE/S007415/1).
1072	
1073	Competing interests
1074	The authors declare that they have no known competing financial interests or personal
1075	relationships that could have appeared to influence the work reported in this paper.
1076	
1077	Data availability
1078	All data generated or analysed during this study are included in this published article (and its
1079	supplementary material files).
1080	
1081	References
1082	Ainsworth, N.R. and Riley, L.A., 2010. Triassic to Middle Jurassic stratigraphy of the Kerr McGee
1083	97/12-1 exploration well, offshore southern England. Marine and Petroleum Geology, 27(4),
1084	pp.853-884. https://doi.org/10.1016/j.marpetgeo.2009.12.014
1085	Ali, A.D., 1982. Triassic stratigraphy and sedimentology in central England (Doctoral dissertation,
1086	Aston University).

1087	AlNajdi, N. and Worden, R.H., 2023. Porosity in mudstones and its effectiveness for sealing carbon
1088	capture and storage sites. Geological Society, London, Special Publications, 528(1), pp.339-
1089	357. https://doi.org/10.1144/SP528-2022-84
1090	Ambrose, K., Hough, E., Smith, N. J. P., and Warrington, G., 2014. Lithostratigraphy of the Sherwood
1091	Sandstone Group of England, Wales and south-west Scotland. British Geological Survey
1092	Research Report, RR/14/01.
1093	Armitage, P.J., Worden, R.H., Faulkner, D.R., Aplin, A.C., Butcher, A.R. and Espie, A.A., 2013. Mercia
1094	Mudstone Formation caprock to carbon capture and storage sites: petrology and petrophysical
1095	characteristics. Journal of the Geological Society, 170(1), pp.119-132.
1096	https://doi.org/10.1144/jgs2012-049
1097	Arthurton, R.S., 1980. Rhythmic sedimentary sequences in the Triassic Keuper Marl (mercia
1098	mudstone group) of Cheshire, northwest England. <i>Geological Journal</i> , 15(1), pp.43-58.
1099	https://doi.org/10.1002/gj.3350150106
1100	Audley-Charles, M.G., 1970. Triassic palaeogeography of the British Isles. Quarterly Journal of the
1101	Geological Society, 126(1-4), pp.49-74. https://doi.org/10.1144/gsjgs.126.1.0049
1102	Augustsson, C., Voigt, T., Bernhart, K., Kreißler, M., Gaupp, R., Gärtner, A., Hofmann, M. and
1103	Linnemann, U., 2018. Zircon size-age sorting and source-area effect: The German Triassic
1104	Buntsandstein Group. Sedimentary Geology, 375, pp.218-231.
1105	https://doi.org/10.1016/j.sedgeo.2017.11.004
1106	Augustsson, C., 2021. Influencing factors on petrography interpretations in provenance research—a
1107	case-study review. Geosciences, 11(5), p.205. https://doi.org/10.3390/geosciences11050205
1108	Baptiste, J., 2016. Cartographie structurale et lithologique du substratum du Bassin parisien et sa
1109	place dans la chaîne varisque de l'Europe de l'Ouest: approches combinées géophysiques,
1110	pétrophysiques, géochronologiques et modélisations 2D (Doctoral dissertation, Université
1111	d'Orléans).
1112	Barclay, W J, Ambrose, K, Chadwick, R A, and Pharaoh T C. 1997. Geology of the country around
1113	Worcester. Memoir of the British Geological Survey, Sheet 199 (England and Wales).

1114	Basu, A., 1976. Petrology of Holocene fluvial sand derived from plutonic source rocks; implications to
1115	paleoclimatic interpretation. Journal of Sedimentary Research, 46(3), pp.694-709.
1116	https://doi.org/10.1306/212F7031-2B24-11D7-8648000102C1865D
1117	Benabdellouahed, M., Dugué, O., Tessier, B., Thinon, I., Guennoc, P. and Bourdillon, C., 2014.
1118	Nouvelle cartographie du substratum de la baie de Seine et synthèse géologique terre-mer:
1119	apports de nouvelles données sismiques et biostratigraphiques. Géologie de la France, 1(2),
1120	pp.21-25.
1121	Bourquin, S., Bercovici, A., López-Gómez, J., Diez, J.B., Broutin, J., Ronchi, A., Durand, M., Arché, A.
1122	Linol, B. and Amour, F., 2011. The Permian–Triassic transition and the onset of Mesozoic
1123	sedimentation at the northwestern peri-Tethyan domain scale: palaeogeographic maps and
1124	geodynamic implications. Palaeogeography, Palaeoclimatology, Palaeoecology, 299(1-2),
1125	pp.265-280. https://doi.org/10.1016/j.palaeo.2010.11.007
1126	Bowman, M.B.J., McClure, N.M. and Wilkinson, D.W., 1993. Wytch Farm oilfield: deterministic
1127	reservoir description of the Triassic Sherwood Sandstone. In Geological Society, London,
1128	Petroleum Geology Conference Series (Vol. 4, No. 1, pp. 1513-1517). The Geological Society
1129	of London. https://doi.org/10.1144/0041513
1130	Bray, R.J., Duddy, I.R. and Green, P.F., 1998. Multiple heating episodes in the Wessex Basin:
1131	implications for geological evolution and hydrocarbon generation. Geological Society, London,
1132	Special Publications, 133(1), pp.199-213. https://doi.org/10.1144/GSL.SP.1998.133.01.09
1133	Bridge, D McC, Carney, J N, Lawley, R S, and Rushton, A W A. 1998. Geology of the country around
1134	Coventry and Nuneaton. Memoir of the British Geological Survey, sheet 169 (England and
1135	Wales).
1136	Bridge, D McC, and Hough, E. 2002. Geology of the Wolverhampton and Telford district. Sheet
1137	description of the British Geological Survey, 1:50 000 Series Sheet 153 (England and Wales).
1138	Brookfield, M.E., 2008. Palaeoenvironments and palaeotectonics of the arid to hyperarid
1139	intracontinental latest Permian-late Triassic Solway basin (UK). Sedimentary Geology, 210(1-
1140	2), pp.27-47. https://doi.org/10.1016/j.sedgeo.2008.06.003

1141	Buchanan, J.G., 1998. The exploration history and controls on hydrocarbon prospectivity in the
1142	Wessex basins, southern England, UK. Geological Society, London, Special
1143	Publications, 133(1), pp.19-37. https://doi.org/10.1144/GSL.SP.1998.133.01.02
1144	Burgess, P.M., Dobromylskyj, E. and Lovell-Kennedy, J., 2025. Probably proximal pebbles? An
1145	outcrop-constrained quantitative analysis of clast transport distances in the lower Triassic
1146	Sherwood Sandstone Group, UK. Journal of the Geological Society, 182(3), pp.jgs2024-155.
1147	https://doi.org/10.1144/jgs2024-155
1148	Burley, S.D., 1984. Patterns of diagenesis in the Sherwood sandstone group (Triassic), United
1149	Kingdom. Clay Minerals, 19(3), pp.403-440. https://doi.org/10.1180/claymin.1984.019.3.11
1150	Burley, S.D., 1987. Diagenetic modelling in the Triassic Sherwood sandstone group of England and its
1151	offshore equivalents, United Kingdom continental shelf (Doctoral dissertation, University of
1152	Hull).
1153	Busby, J.P. and Smith, N.J.P., 2001. The nature of the Variscan basement in southeast England:
1154	evidence from integrated potential field modelling. <i>Geological Magazine</i> , 138(6), pp.669-685.
1155	https://doi.org/10.1017/S0016756801005751
1156	Bushell, T.P., 1986. Reservoir geology of the Morecambe Field. <i>Geological Society, London, Special</i>
1157	Publications, 23(1), pp.189-208. https://doi.org/10.1144/GSL.SP.1986.023.01.12
1158	Butler, M., 1998. The geological history of the southern Wessex Basin—a review of new information
1159	from oil exploration. Geological Society, London, Special Publications, 133(1), pp.67-86.
1160	https://doi.org/10.1144/GSL.SP.1998.133.01.04
1161	Butler, M. 2019, Seismostratigraphic analysis of Paleozoic sequences of the Midlands
1162	Microcraton. Geological Society, London, Special Publications 471, no. 1: 317-332.
1163	https://doi.org/10.1144/SP471.6
1164	Carter, A., Yelland, A., Bristow, C. and Hurford, A.J., 1995. Thermal histories of Permian and Triassic
1165	basins in Britain derived from fission track analysis. Geological Society, London, Special
1166	Publications, 91(1), pp.41-56. https://doi.org/10.1144/GSL.SP.1995.091.01.03

116/	Castellfort, S., Fillon, C., Lasseur, E, Ortiz, A., Robin, C., Guillocheau, F., Tremblin, M., Bessin, P.,
1168	Guerit, L., Dekoninck, A., Allanic, C., Gautheron, C., Barbarand, J., Loget, N., Uzel, J., Yans, J.,
1169	Briais, J., Al-Reda, M., Baby, G., François, T., Roig, J. & Calassou, S. (2023). The Source-to-
1170	Sink Vade-mecum: History, Concepts and Tools. Society for Sedimentary Geology. CSP 16.
1171	https://doi.org/10.2110/sepmcsp.16
1172	Chadwick, R.A. and Evans, D.J., 1995. The timing and direction of Permo-Triassic extension in
1173	southern Britain. Geological Society, London, Special Publications, 91(1), pp.161-192.
1174	https://doi.org/10.1144/GSL.SP.1995.091.01.09
1175	Chadwick, R. A., Jackson, D. I., Barnes, Kimbell, G. S., Johnson, H., Chiverrell, R. C., Thomas, G. S.
1176	P., Jones, N. S., Riley N. J., Pickett, E. A., Young, B., Holliday, D. W., Ball, D. F., Molyneux, S.,
1177	Long, D., Power, G. M., and Roberts, D., 2001. Geology of the Isle of Man and its offshore
1178	area. (Keyworth, Nottingham: British Geological Survey and Treasury Isle of Man.)
1179	Charsley, T. J., 1982. A standard nomenclature for the Triassic formations of the Ashbourne district.
1180	Report of the Institute of Geological Sciences, 81/14
1181	Chedburn, L., Underhill, J.R., Head, S. and Jamieson, R., 2022. The critical evaluation of carbon
1182	dioxide subsurface storage sites: Geological challenges in the depleted fields of Liverpool
1183	Bay. AAPG bulletin, 106(9), pp.1753-1789. https://doi.org/10.1306/07062221120
1184	Chisholm, J. I., Charsley, T. J. And Aitkenhead, N. 1988. Geology of the country around Ashbourne
1185	and Cheadle. Memoir of the British Geological Survey, Sheet 124.
1186	Cosgrove, G.I., Alkathery, M., Al-Masrahy, M., Colombera, L., Mountney, N.P. and Thompson, D.B.,
1187	2025. Quantitative sedimentological analysis of the aeolian–fluvial Triassic Sherwood
1188	Sandstone Group, Cheshire Basin, UK. Sedimentology, 72(4), pp.1233-1274.
1189	https://doi.org/10.1111/sed.70000
1190	Costelloe, J.F., Grayson, R.B. and McMahon, T.A., 2006. Modelling streamflow in a large
1191	anastomosing river of the arid zone, Diamantina River, Australia. Journal of Hydrology, 323(1-
1192	4), pp.138-153. https://doi.org/10.1016/j.jhydrol.2005.08.022

1193	Cowan, G., 1993. Identification and significance of aeolian deposits within the dominantly fluvial
1194	Sherwood Sandstone Group of the East Irish Sea Basin UK. Geological Society, London,
1195	Special Publications, 73(1), pp.231-245. https://doi.org/10.1144/GSL.SP.1993.073.01.14
1196	Croker, P. and Shannon, P. 1987. The evolution and hydrocarbon prospectivity of the Porcupine
1197	Basin, offshore Ireland. Conference on Petroleum Geology of North West Europe. Barbican
1198	Centre, London, 26-29 October, 3, pp.633-642.
1199	De Sainz Simpson, R., 2022. Sherwood Sandstone Outcrop Analogues Study in the Cheshire Basin:
1200	How to Better Constrain CCS Potential and Co2 Injectability in Depleted Oil and Gas Fields in
1201	the Context of the Liverpool Bay Carbon Capture Project (Master's thesis, The University of
1202	Manchester (United Kingdom)).
1203	Dercourt, J., Gaetani, M., Vrielynck, B., Barrier, E., Biju-Duval, B., Brunet, M.F., Cadet, J.P., Crasquin
1204	S., Sandulescu, M., 2000. Atlas Peri-Tethys - Paleogeographical maps. CCGM / CGMW Paris.
1205	DiGRock250k [SHAPE geospatial data], Scale 1:250000, Tiles: GB, Updated: 31 December 2013,
1206	BGS, Using: EDINA Geology Digimap Service, https://digimap.edina.ac.uk , Downloaded:
1207	2024-07-17 23:35:57.305
1208	DiGRock625k [SHAPE geospatial data], Scale 1:625000, Tiles: GB, Updated: 31 December 2008,
1209	BGS, Using: Ordinance Survey, https://osdatahub.os.uk/ , Downloaded: 2023-11-23
1210	13:34:58.
1211	Donato, J.A., Pullan, C.P. and Dimitropoulos, K., 2023. Moho topography beneath England, the
1212	regional gravity field and speculations on crustal structure. UK Onshore Geophysical Library
1213	Downing, R.A., Allen, D.J., Barker, J.A., Burgess, W.G., Gray, D.A., Price, M. and Smith, I.F., 1984.
1214	Geothermal exploration at Southampton in the UK: a case study of a low enthalpy
1215	resource. Energy exploration & exploitation, 2(4), pp.327-342.
1216	https://doi.org/10.1177/014459878400200404
1217	Dunford, G.M., Dancer, P.N. and Long, K.D., 2001. Hydrocarbon potential of the Kish Bank Basin:
1218	integration within a regional model for the Greater Irish Sea Basin. Geological Society, London
1219	Special Publications, 188(1), pp.135-154. https://doi.org/10.1144/GSL.SP.2001.188.01.07

1220	Earp, J. R. and Taylor, B. J. 1986. Geology of the country around Chester and Winsford. Memoir
1221	British Geological Survey, Sheet 109 (England and Wales).
1222	English, K.L., English, J.M., Moscardini, R., Haughton, P.D., Raine, R.J. and Cooper, M., 2024.
1223	Review of Triassic Sherwood Sandstone Group reservoirs of Ireland and Great Britain and their
1224	future role in geoenergy applications. Geoenergy, 2(1), pp.geoenergy2023-042.
1225	https://doi.org/10.1144/geoenergy2023-042
1226	Evans, D.J. and Holloway, S., 2009. A review of onshore UK salt deposits and their potential for
1227	underground gas storage. Geological Society, London, Special Publications, 313(1), pp.39-80.
1228	https://doi.org/10.1144/SP313.5
1229	Evans, D.J., Rees, J.G. and Holloway, S., 1993. The Permian to Jurassic stratigraphy and structural
1230	evolution of the central Cheshire Basin. <i>Journal of the Geological Society</i> , 150(5), pp.857-870.
1231	https://doi.org/10.1144/gsjgs.150.5.0857
1232	Evans, D.J., Williams, J.D.O., Hough, E. and Stacey, A., 2011. The stratigraphy and lateral
1233	correlations of the Northwich and Preesall halites from the Cheshire Basin-East Irish Sea
1234	areas: implications for sedimentary environments, rates of deposition and the solution mining of
1235	gas storage caverns. In: SMRI Fall 2011 Technical Conference, York, UK, 2-4 Oct 2011.
1236	Floodpage, J., Newman, P., White, J., 2001. Hydrocarbon prospectivity in the Irish Sea area: Insights
1237	from recent exploration of the Central Irish Sea, Peel and Solway basins. In: The Petroleum
1238	Exploration of Ireland's Offshore Basins, P. M. Shannon, P. D. W. Haughton, D. V. Corcoran
1239	(eds). The Petroleum Exploration of Ireland's Offshore Basins. Geological Society, London,
1240	Special Publications, 188, 107-134. https://doi.org/10.1144/GSL.SP.2001.188.01.06
1241	Franklin, J., Tyrrell, S., O'Sullivan, G., Nauton-Fourteu, M. and Raine, R., 2020. Provenance of
1242	Triassic sandstones in the basins of Northern Ireland—Implications for NW European Triassic
1243	palaeodrainage. Geological Journal, 55(7), pp.5432-5450. https://doi.org/10.1002/gj.3697
1244	Garzanti, E., 2019. Petrographic classification of sand and sandstone. Earth-science reviews, 192,
1245	pp.545-563. https://doi.org/10.1016/j.earscirev.2018.12.014
1246	Gent, C.M.A., 2016. Maturity modelling of well 110/07b- 6. British Geological Survey Commissioned
1247	Report, CR/16/043. 25pp.

1248	Gibson-Poole, C.M., Tarasewicz, J., Gray, E., Hitchen, K., Bouffin, N., Taplin, M., Gillespie, A. and
1249	Buchanan, S.K., 2026. Endurance saline aquifer CO2 store–from appraisal to development and
1250	beyond. In: Geological Society, London, Energy Geoscience Conference Series (Vol. 1, No. 1,
1251	pp. egc1-2024). The Geological Society of London. https://doi.org/10.1144/egc1-2024-23
1252	Glover, B.W. and Powell, J.H., 1996. Interaction of climate and tectonics upon alluvial architecture:
1253	Late Carboniferous-Early Permian sequences at the southern margin of the Pennine Basin,
1254	UK. Palaeogeography, Palaeoclimatology, Palaeoecology, 121(1-2), pp.13-34.
1255	https://doi.org/10.1016/0031-0182(95)00050-X
1256	Green, P.F., Thomson, K. and Hudson, J.D., 2001. Recognition of tectonic events in undeformed
1257	regions: contrasting results from the Midland Platform and East Midlands Shelf, Central
1258	England. Journal of the Geological Society, 158(1), pp.59-73.
1259	https://doi.org/10.1144/jgs.158.1.59
1260	Hallsworth, C.R., Morton, A.C., Claoué-Long, J. and Fanning, C.M., 2000. Carboniferous sand
1261	provenance in the Pennine Basin, UK: constraints from heavy mineral and detrital zircon age
1262	data. Sedimentary Geology, 137(3-4), pp.147-185. https://doi.org/10.1016/S0037-
1263	0738(00)00153-6
1264	Hamblin, R J O, Crosby, A, Balson, P S, Jones, S M, Chadwick, R A, Penn, I E, And Arthur, M J. 1992.
1265	United Kingdom offshore regional report. The geology of the English Channel, London: HMSO
1266	for the British Geological Survey
1267	Hampson, G. J., Duller, R. A., Petter, A. L., Robinson, R. A. J. & Allen, P. A. (2014) Mass-Balance
1268	Constraints On Stratigraphic Interpretation of Linked Alluvial-Coastal-Shelf Deposits From
1269	Source To Sink: Example From Cretaceous Western Interior Basin, Utah and Colorado, U.S.A.
1270	Journal of Sedimentary Research. 84 (11), 935–960. https://doi.org/10.2110/jsr.2014.78
1271	Hawkes, P.W., Fraser, A.J. and Einchcomb, C.C.G., 1998. The tectono-stratigraphic development and
1272	exploration history of the Weald and Wessex basins, Southern England, UK. Geological
1273	Society, London, Special Publications, 133(1), pp.39-65.
1274	https://doi.org/10.1144/GSL.SP.1998.133.01.03

1275	Head, S., Underhill, J.R., Jamieson, R. and Busch, A., 2026, April. Evaluating the role of cap rock in
1276	controlling natural accumulation and storage of carbon dioxide in the East Irish Sea Basin, UK.
1277	In Geological Society, London, Energy Geoscience Conference Series (Vol. 1, No. 1, pp. egc1-
1278	2024). The Geological Society of London. https://doi.org/10.1144/egc1-2024-10
1279	Helland-Hansen, W., Sømme, T. O., Martinsen, O. J., Lunt, I. & Thurmond, J. (2016) Deciphering
1280	Earth's natural hourglasses; perspectives on source-to-sink analysis. Journal of Sedimentary
1281	Research. 86 (9), 1008-1033. https://doi.org/10.2110/jsr.2016.56
1282	Herries, R.D. and Cowan, G., 1997. Challenging the 'sheetflood'myth: the role of water-table-
1283	controlled sabkha deposits in redefining the depositional model for the Ormskirk Sandstone
1284	Formation (Lower Triassic), East Irish Sea Basin. Geological Society, London, Special
1285	Publications, 124(1), pp.253-276. https://doi.org/10.1144/GSL.SP.1997.124.01.16
1286	Holliday, D.W., Williams, G.M., Holloway S., Savage D. and Bannon M.P, 1991. A Preliminary
1287	Feasibility Study for the Underground Disposal of Carbon Dioxide in UK. Nottingham, UK,
1288	British Geological Survey, 32pp. (WE/91/020) (Unpublished)
1289	Hounslow, M.W. and McIntosh, G., 2003. Magnetostratigraphy of the Sherwood Sandstone Group
1290	(Lower and Middle Triassic), south Devon, UK: detailed correlation of the marine and non-
1291	marine Anisian. Palaeogeography, Palaeoclimatology, Palaeoecology, 193(2), pp.325-348.
1292	https://doi.org/10.1016/S0031-0182(03)00235-9
1293	Hounslow, M.W., McIntosh, G., Edwards, R.A., Laming, D.J. and Karloukovski, V., 2017. End of the
1294	Kiaman Superchron in the Permian of SW England: magnetostratigraphy of the Aylesbeare
1295	Mudstone and Exeter groups. Journal of the Geological Society, 174(1), pp.56-74.
1296	https://doi.org/10.1144/jgs2015-141
1297	Hounslow, M.W. and Gallois, R., 2023. Magnetostratigraphy of the Mercia Mudstone Group (Devon,
1298	UK): implications for regional relationships and chronostratigraphy in the Middle to Late Triassic
1299	of Western Europe. Journal of the Geological Society, 180(4), pp.jgB2022-173.
1300	https://doi.org/10.1144/jgs2022-173

1301	Howard, A S, Warrington, G, Ambrose, K, and Rees, J G. 2008. A formational framework for the
1302	Mercia Mudstone Group (Triassic) of England and Wales. British Geological Survey Research
1303	Report, RR/08/04.
1304	Howard, A., Warrington, G., Carney, J., Ambrose, K., Young, S.R., Pharaoh, T. and Cheney, C.,
1305	2009. Geology of the Nottingham district: memoir for 1: 50 000 geological sheet 126 (England
1306	and Wales). British Geological Survey.
1307	Husein, S.S., Roberts, G.G., Fraser, A. and Bell, R., 2025. Unravelling the Nature and Origin of
1308	Jurassic to Early Cretaceous Unconformities Offshore Southwest Britain. Basin Research, 37,
1309	p.e70026. https://doi.org/10.1111/bre.70026
1310	Ingersoll, R., Bullard, T., Ford, R.L., Grimm, J.P., Pickle, J.D. and Sares, S.W., 1984. The effect of
1311	grain size on detrital modes: a test of the Gazzi- Dickinson point-counting method (Holocene,
1312	sand, New Mexico, USA). Journal of Sedimentary Petrology. 54. 103-116.
1313	https://doi.org/10.1306/212F83B9-2B24-11D7-8648000102C1865D
1314	Ireland, R.J., Pollard, J.E., Steel, R.J. and Thompson, D.B., 1978. Intertidal sediments and trace
1315	fossils from the Waterstones (Scythian-Anisian?) at Daresbury, Cheshire. Proceedings of the
1316	Yorkshire Geological Society, 41(4), pp.399-436. https://doi.org/10.1144/pygs.41.4.399
1317	Jackson, D. I., Jackson, A. A., Evans, D., Wingfield, R. T. R., Barnes, R. P., and Arthur, M. J., 1995.
1318	United Kingdom offshore regional report: the geology of the Irish Sea. (London: HMSO for the
1319	British Geological Survey.)
1320	Jackson, D.I., Johnson, H. and Smith, N.J.P., 1997. Stratigraphical relationships and a revised
1321	lithostratigraphical nomenclature for the Carboniferous, Permian and Triassic rocks of the
1322	offshore East Irish Sea Basin. Geological Society, London, Special Publications, 124(1), pp.11-
1323	32. https://doi.org/10.1144/GSL.SP.1997.124.01.02
1324	Jeans, C.V., 2006. Clay mineralogy of the Permo-Triassic strata of the British Isles: onshore and
1325	offshore. Clay Minerals, 41(1), pp.309-354. https://doi.org/10.1180/0009855064110199
1326	Jefferson, I., Rosenbaum, M. and Smalley, I., 2002. Mercia Mudstone as a Triassic aeolian desert
1327	sediment. Mercian Geologist, 15(3), pp.157-162.

1328	Jones, N.S. and Ambrose, K., 1994. Triassic sandy braidplain and aeolian sedimentation in the
1329	Sherwood Sandstone Group of the Sellafield area, west Cumbria. Proceedings of the Yorkshire
1330	Geological Society, 50(1), pp.61-76. https://doi.org/10.1144/pygs.50.1.61
1331	Jones, N.S., Holliday, D.W. and McKERVEY, J.A., 2011. Warwickshire Group (Pennsylvanian) red-
1332	beds of the Canonbie Coalfield, England-Scotland border, and their regional
1333	palaeogeographical implications. Geological Magazine, 148(1), pp.50-77.
1334	https://doi.org/10.1017/S001675681000035X
1335	Jones, S.T., Worden, R.H., Faulkner, D.R., Fisher, Q.J., McEvoy, J.A. and Utley, J.E., 2025.
1336	Deposition, diagenesis, and porosity of a siliciclastic caprock: the Late Triassic Mercia
1337	Mudstone Group. Journal of the Geological Society, pp.jgs2025-086.
1338	https://doi.org/10.1144/jgs2025-086
1339	Knox, R.O.B., Burgess, W.G., Wilson, K.S. and Bath, A.H., 1984. Diagenetic influences on reservoir
1340	properties of the Sherwood Sandstone (Triassic) in the Marchwood geothermal borehole,
1341	Southampton, UK. Clay Minerals, 19(3), pp.441-456.
1342	https://doi.org/10.1180/claymin.1984.019.3.12
1343	Lang, S.C., Payenberg, T.H.D., Reilly, M.R.W., Hicks, T., Benson, J. and Kassan, J., 2004. Modern
1344	analogues for dryland sandy fluvial-lacustrine deltas and terminal splay reservoirs. The APPEA
1345	Journal, 44(1), pp.329-356. https://doi.org/10.1071/AJ03012
1346	Mange, M., Turner, P., Ince, D., Pugh, J. and Wright, D., 1999. A new perspective on the zonation and
1347	correlation of barren strata: an integrated heavy mineral and palaeomagnetic study of the
1348	Sherwood Sandstone Group, East Irish Sea Basin and surrounding areas. Journal of Petroleum
1349	Geology, 22(3), pp.325-348. https://doi.org/10.1111/j.1747-5457.1999.tb00990.x
1350	Mange, M.A., Turner, P., Ince, D. and Wright, D.T., 2007. High-resolution heavy mineral-and
1351	magnetostratigraphy; a powerful tool for subdivision and correlation of barren successions: An
1352	example from the Sherwood Sandstone Group (Triassic) of the East Irish Sea Basin and
1353	surrounding areas. Developments in Sedimentology, 58, pp.1073-1097.
1354	https://doi.org/10.1016/S0070-4571(07)58042-8

1355	Mao, X., Liu, X. and Zhou, X., 2021. Permo-Triassic aeolian red clay of southwestern England and its
1356	palaeoenvironmental implications. Aeolian Research, 52, p.100726.
1357	https://doi.org/10.1016/j.aeolia.2021.100726
1358	Markwick, P. J. (2019) Palaeogeography in exploration. Geological Magazine. 156 (2), 366-407.
1359	https://doi.org/10.1017/S0016756818000468
1360	Marsh, J.R., Jones, S.J., Meadows, N.S. and Gluyas, J.G., 2022. Petrographic and diagenetic
1361	investigation of the distal Triassic 'Budleighensis' fluvial system in the Solway and Carlisle
1362	Basins for potential CO2 storage. Petroleum Geoscience, 28(3), pp.petgeo2021-065.
1363	https://doi.org/10.1144/petgeo2021-065
1364	Martínez Catalán, J.R., Schulmann, K. and Ghienne, J.F., 2021. The Mid-Variscan Allochthon: Keys
1365	from correlation, partial retrodeformation and plate-tectonic reconstruction to unlock the
1366	geometry of a non-cylindrical belt. Earth-Science Reviews, 220, p.103700.
1367	https://doi.org/10.1016/j.earscirev.2021.103700
1368	Marx, S.K., May, J-H., Cohen. T., Kamber. B.S., McGowan, H.A. and Petherick L. (2022). Dust
1369	emissions from Kati Thanda-Lake Eyre: a review. Transactions of the Royal Society of South
1370	Australia, 146:1, 168-206, https://doi.org/10.1080/03721426.2022.2054918
1371	McKie, T., Aggett, J. and Hogg, A.J.C., 1997. Sequence architecture of a Triassic semi-arid, fluvio-
1372	lacustrine reservoir, Wytch Farm Field, southern England. In: GCSSEPM Foundation 18th
1373	Annual Research Conference Shallow Marine and Nonmarine Reservoirs, December 7-10,
1374	1997. https://doi.org/10.5724/gcs.97.18.0197
1375	Mckie, T., 2011. A comparison of modern Dryland depositional systems with the Rotliegend group in
1376	the Netherlands. SEPM Special Publications. 98. 89-103.
1377	https://doi.org/10.2110/pec.11.98.0089.
1378	Mckie, T., 2014. Climatic and tectonic controls on Triassic dryland terminal fluvial system architecture,
1379	central North Sea. In: Martinius, A.W., Ravnås, R., Howell, J.A., Steel, R.J. and Wonham, J.P.
1380	(eds) From Depositional Systems to Sedimentary Successions on the Norwegian Continental
1381	Shelf. Blackwell, Oxford, 46, 19–58 [IAS Special Publication].
1382	https://doi.org/10.1002/9781118920435.ch2

1383	McKie, I., 2017. Palaeogeographic evolution of latest Permian and Triassic salt basins in Northwest
1384	Europe. In: Soto, J. I., Flinch, J. F. and Tari, G. (eds.) Permo-triassic salt provinces of Europe,
1385	North Africa and the Atlantic margins (pp. 159-173). Elsevier. https://doi.org/10.1016/B978-0-
1386	12-809417-4.00008-2
1387	Meadows, N.S., 2006. The correlation and sequence architecture of the Ormskirk sandstone
1388	formation in the Triassic Sherwood sandstone group of the East Irish Sea Basin, NW
1389	England. Geological Journal, 41(1), pp.93-122. https://doi.org/10.1002/gj.1034
1390	Meadows, N. S., Director at Redrock Associates Int Ltd (Personal communication, 3rd March 2025)
1391	Meadows, N.S. and Beach, A., 1993a. Controls on reservoir quality in the Triassic Sherwood
1392	Sandstone of the Irish Sea. In Geological Society, London, Petroleum Geology Conference
1393	Series (Vol. 4, No. 1, pp. 823-833). The Geological Society of London.
1394	https://doi.org/10.1144/0040823
1395	Meadows, N.S. and Beach, A., 1993b. Structural and climatic controls on facies distribution in a mixed
1396	fluvial and aeolian reservoir: the Triassic Sherwood Sandstone in the Irish Sea. Geological
1397	Society, London, Special Publications, 73(1), pp.247-264.
1398	https://doi.org/10.1144/GSL.SP.1993.073.01.15
1399	Medici, G., West, L.J. and Mountney, N.P., 2019a. Sedimentary flow heterogeneities in the Triassic
1400	UK Sherwood Sandstone Group: insights for hydrocarbon exploration. Geological
1401	Journal, 54(3), pp.1361-1378. https://doi.org/10.1002/gj.3233
1402	Medici, G., West, L.J., Mountney, N.P. and Welch, M., 2019b. Permeability of rock discontinuities and
1403	faults in the Triassic Sherwood Sandstone Group (UK): insights for management of fluvio-
1404	aeolian aquifers worldwide. Hydrogeology Journal, 27(8), pp.2835-2855.
1405	https://doi.org/10.1007/s10040-019-02035-7
1406	Mikkelsen, P.W. and Floodpage, J.B., 1997. The hydrocarbon potential of the Cheshire
1407	Basin. Geological Society, London, Special Publications, 124(1), pp.161-183.
1408	https://doi.org/10.1144/GSL.SP.1997.124.01.10
1409	Merlin Energy Resources Consortium, 2020. The Standard Stratigraphic Nomenclature of Offshore
1410	Ireland: An Integrated Lithostratigraphic, Biostratigraphic and Sequence Stratigraphic

1411	Framework. Project Atlas. Petroleum Affairs Division, Department of the Environment (DEEC),
1412	Climate and Communications, Special Publication, 1/21.
1413	Michael, N.A. and Zühlke, R., 2022. Source-to-sink: Regional grain size trends to reconstruct
1414	sediment budgets and catchment areas. Basin Research, 34(1), pp.393-410.
1415	https://doi.org/10.1111/bre.12624
1416	Miliorizos, M. and Ruffell, A., 1998. Kinematics of the Watchet-Cothelstone-Hatch fault system:
1417	implications for the fault history of the Wessex basin and adjacent areas. Geological Society,
1418	London, Special Publications, 133(1), pp.311-330.
1419	https://doi.org/10.1144/GSL.SP.1998.133.01.15
1420	Morón, S., Amos, K. and Mann, S., 2014. Fluvial reservoirs in dryland endorheic basins: the Lake
1421	Eyre Basin as a world-class modern analogue. The APPEA Journal, 54(1), pp.119-134.
1422	https://doi.org/10.1071/AJ13014
1423	Morton, A.C., Chisholm, J.I. and Frei, D., 2021. Provenance of Carboniferous sandstones in the
1424	central and southern parts of the Pennine Basin, UK: evidence from detrital zircon
1425	ages. Proceedings of the Yorkshire Geological Society, 63(3), pp.pygs2020-010.
1426	https://doi.org/10.1144/pygs2020-010
1427	Morton, A.C., Chisholm, J.I. and Frei, D., 2024. Provenance response to evolving palaeogeography
1428	recorded by Carboniferous sandstones in the northern Pennine Basin, UK. Sedimentary
1429	Geology, 470, p.106691. https://doi.org/10.1016/j.sedgeo.2024.106691
1430	Morton, A.C. and Hallsworth, C., 1994. Identifying provenance-specific features of detrital heavy
1431	mineral assemblages in sandstones. Sedimentary Geology, 90(3-4), pp.241-256.
1432	https://doi.org/10.1016/0037-0738(94)90041-8
1433	Morton, A., Hounslow, M.W. and Frei, D., 2013. Heavy-mineral, mineral-chemical and zircon-age
1434	constraints on the provenance of Triassic sandstones from the Devon coast, southern
1435	Britain. <i>Geologos</i> , 19(1-2), pp.67-85. https://doi.org/10.2478/logos-2013-0005
1436	Morton, A., Knox, R. and Frei, D., 2016. Heavy mineral and zircon age constraints on provenance of
1437	the Sherwood Sandstone Group (Triassic) in the eastern Wessex Basin, UK. Proceedings of
1438	the Geologists' Association, 127(4), pp.514-526. https://doi.org/10.1016/j.pgeola.2016.06.001

1439	Mountney, N.P. and Thompson, D.B., 2002. Stratigraphic evolution and preservation of aeolian dune
1440	and damp/wet interdune strata: an example from the Triassic Helsby Sandstone Formation,
1441	Cheshire Basin, UK. Sedimentology, 49(4), pp.805-833. https://doi.org/10.1046/j.1365-
1442	3091.2002.00472.x
1443	Naylor, D., Haughey, N., Clayton, G. and Graham, J.R., 1993. The Kish Bank Basin, offshore Ireland.
1444	In Geological Society, London, Petroleum Geology Conference Series (Vol. 4, No. 1, pp. 845-
1445	855). The Geological Society of London. https://doi.org/10.1144/0040845
1446	Newell, A. J., 2017a. Rifts, rivers and climate recovery: A new model for the Triassic of
1447	England. Proceedings of the Geologists' Association, 129(3), pp.352-371.
1448	https://doi.org/10.1016/j.pgeola.2017.04.001
1449	Newell, A. J., 2017b. Evolving stratigraphy of a Middle Triassic fluvial-dominated sheet sandstone:
1450	The Otter Sandstone Formation of the Wessex Basin (UK). Geological Journal, 53(5), pp.1954-
1451	1972. https://doi.org/10.1002/gj.3026
1452	Newell, A. J., 2023 The Sherwood Sandstone and Bacton groups of the East Midlands Shelf – an
1453	onshore to offshore correlation using outcrop evidence and geophysical logs. Nottingham, UK,
1454	British Geological Survey.
1455	Newell, A. 2024. UK Stratigraphical Framework Series: Mercia Mudstone Group. British Geological
1456	Survey Open Report, OR/24/046. 77pp.
1457	Newell, A.J. and Shariatipour, S.M., 2016. Linking outcrop analogue with flow simulation to reduce
1458	uncertainty in sub-surface carbon capture and storage: an example from the Sherwood
1459	Sandstone Group of the Wessex Basin, UK. Geological Society, London, Special
1460	Publications, 436(1), pp.231-246. https://doi.org/10.1144/SP436
1461	Newell, A J, Smith, N J., 2009. Bromsgrove Aquifer Groundwater Modelling Study: Results from Task
1462	1.1 3D Visualisation and Geological Framework of the Bromsgrove Aquifer. British Geological
1463	Survey Commissioned Report, CR/09/023. 18pp.
1464	Newman, P.J., 1999. The geology and hydrocarbon potential of the Peel and Solway Basins, East
1465	Irish Sea. Journal of Petroleum Geology, 22(3), pp.305-324. https://doi.org/10.1111/j.1747-
1466	5457.1999.tb00989.x

Gradstein, F. M., Ogg, J. G., Schmitz, M. D., Ogg G. M., Geologic Time Scale, (pp. 903-953) Elsevier, https://doi.org/10.1016/B978-0-12-824360-2.00025-5. R. A., Sumbler, M. G. and Ambrose, K. 1987. Geology of the country around Warwick. <i>Memoir of the British Geological Survey</i> , Sheet 184 (England & Wales). R. A., Hamblin, R. J. O., Ambrose, K., and Warrington, G. 1991. Geology of the country around Redditch. Memoir of the British Geological Survey, Sheet 183 (England and Wales). a, C., Martin, J. M., 2012. Mass-Balance Effects In Depositional Systems. <i>Journal of Sedimentary</i>
 R. A., Sumbler, M. G. and Ambrose, K. 1987. Geology of the country around Warwick. <i>Memoir of the British Geological Survey</i>, Sheet 184 (England & Wales). R A, Hamblin, R J O, Ambrose, K, and Warrington, G. 1991. Geology of the country around Redditch. Memoir of the British Geological Survey, Sheet 183 (England and Wales).
the British Geological Survey, Sheet 184 (England & Wales). R A, Hamblin, R J O, Ambrose, K, and Warrington, G. 1991. Geology of the country around Redditch. Memoir of the British Geological Survey, Sheet 183 (England and Wales).
R A, Hamblin, R J O, Ambrose, K, and Warrington, G. 1991. Geology of the country around Redditch. Memoir of the British Geological Survey, Sheet 183 (England and Wales).
Redditch. Memoir of the British Geological Survey, Sheet 183 (England and Wales).
a, C., Martin, J. M., 2012. Mass-Balance Effects In Depositional Systems. <i>Journal of Sedimentary</i>
Research, 82 (6), pp.435–450. https://doi.org/10.2110/jsr.2012.38
es, D., Busby, J., Kemp, S.J., Petitclerc, E. and Mounteney, I., 2021. The thermal properties of
the Mercia Mudstone Group. Quarterly Journal of Engineering Geology and
Hydrogeology, 54(2), pp.qjegh2020-098. https://doi.org/10.1144/qjegh2020-098
, J., Wemmer, K. and Ahrendt, H., 2008. Provenance of siliciclastic sediments (Permian to
Jurassic) in the Central European Basin. Zeitschrift der Deutschen Gesellschaft fur
Geowissenschaften, 159(4), pp.641-650. https://doi.org/10.1127/1860-1804/2008/0159-0641
n, S., Bourquin, S., Fluteau, F. and Guillocheau, F., 2005. Paleoenvironment reconstructions and
climate simulations of the Early Triassic: impact of the water and sediment supply on the
preservation of fluvial systems. <i>Geodinamica Acta</i> , 18(6), pp.431-446.
https://doi.org/10.3166/ga.18.431-446
aoh, T.C., Gent, C.M.A., Hannis, S.D., Kirk, K.L., Monaghan, A.A., Quinn, M.F., Smith, N.J.P.,
Vane, C.H., Wakefield, O. and Waters, C.N., 2019. An overlooked play? Structure, stratigraphy
and hydrocarbon prospectivity of the Carboniferous in the East Irish Sea-North Channel basin
complex. Geological Society, London, Special Publications, 471(1), pp.281-316.
https://doi.org/10.1144/SP471.7
t, J A, Jones, D G, and Haslam, H W (editors). 1999. The Cheshire Basin: Basin evolution, fluid
movement and mineral resources in a Permo-Triassic rift setting. Keyworth, Nottingham: for the
British Geological Survey.

1494	Pullan, C. P., Donato, J. A., 2022. The Eastern Extension of Southwest England under the Mesozoic
1495	Southern England Basin and its Variscan Dextral Translation. UK Onshore Geophysical Library.
1496	Radley, J.D. and Coram, R.A., 2016. The Chester Formation (Early Triassic, southern Britain):
1497	sedimentary response to extreme greenhouse climate?. Proceedings of the Geologists'
1498	Association, 127(5), pp.552-557. https://doi.org/10.1016/j.pgeola.2016.08.002
1499	Ravidà, D.C., Caracciolo, L., Heins, W.A. and Stollhofen, H., 2021. Reconstructing environmental
1500	signals across the Permian-Triassic boundary in the SE Germanic basin: Paleodrainage
1501	modelling and quantification of sediment flux. Global and Planetary Change, 206, p.103632.
1502	https://doi.org/10.1016/j.gloplacha.2021.103631
1503	Rees, J G, and Wilson, A A. 1998. Geology of the country around Stoke-on-Trent. Memoir of the
1504	Geological Survey, Sheet 123 (England and Wales).
1505	Reynolds, T., 2024. Grain size from source to sink-modern and ancient fining rates. <i>Earth-Science</i>
1506	Reviews, 250, p.104699. https://doi.org/10.1016/j.earscirev.2024.104699
1507	Romans, B. W. & Graham, S. A. (2013) A Deep-Time Perspective of Land-Ocean Linkages in the
1508	Sedimentary Record. Annual Review of Marine Science. 5, 69-94.
1509	https://doi.org/10.1146/annurev-marine-121211-172426
1510	Ruffell, A., Coward, M.P. and Harvey, M., 1995. Geometry and tectonic evolution of megasequences
1511	in the Plymouth Bay Basin, English Channel. Geological Society, London, Special Publications,
1512	91(1), pp.193-214. https://doi.org/10.1144/GSL.SP.1995.091.01.10
1513	Sánchez Martínez, S., De la Horra, R., Arenas, R., Gerdes, A., Galán-Abellán, A.B., López-Gómez, J.,
1514	Barrenechea, J.F. and Arche, A., 2012. U-Pb ages of detrital zircons from the Permo-Triassic
1515	series of the Iberian Ranges: a record of variable provenance during rift propagation. The
1516	Journal of Geology, 120(2), pp.135-154. https://doi.org/10.1086/663983
1517	Sass, K., von Eynatten, H., Meyerink, T., Schade, J. and Dunkl, I., 2023. Heavy mineral constraints on
1518	the evolution and provenance of upper Permian and lower Triassic siliciclastic deposits of the
1519	Central European Basin. Journal of Applied & Regional Geology/Zeitschrift der Deutschen
1520	Gesellschaft für Geowissenschaften (ZDGG), 174(3). https://doi.org/10.1127/zdgg/2023/0404

1521	Scorgie, J.C., Worden, R.H., Utley, J.E.P. and Roche, I.P., 2021. Reservoir quality and diagenesis of
1522	Triassic sandstones and siltstones from arid fluvial and playa margin environments: a study of
1523	one of the UK's earliest producing oilfields. Marine and Petroleum Geology, 131, p.105154.
1524	https://doi.org/10.1016/j.marpetgeo.2021.105154
1525	Searle, M.P., Shail, R.K., Pownall, J.M., Jurkowski, C., Watts, A.B. and Robb, L.J., 2024. The Permian
1526	Cornubian granite batholith, SW England; Part 1: Field, structural, and petrological
1527	constraints. Geological Society of America Bulletin, 136(9-10), pp.4301-4320.
1528	https://doi.org/10.1130/B37457.1
1529	Shail, R.K. and Leveridge, B.E., 2009. The Rhenohercynian passive margin of SW England:
1530	Development, inversion and extensional reactivation. Comptes Rendus. Géoscience, 341(2-3),
1531	pp.140-155. https://doi.org/10.1016/j.crte.2008.11.002
1532	Simms, M., 2009. The Permian and Mesozoic. In: Holland, C. H., Sanders, I. (eds). The Geology of
1533	Ireland (pp. 331-332). Liverpool University Press. https://doi.org/10.2307/jj.12638997.16
1534	Smith, S.A. and Edwards, R.A., 1991. Regional sedimentological variations in Lower Triassic fluvial
1535	conglomerates (Budleigh Salterton Pebble Beds), southwest England: some implications for
1536	palaeogeography and basin evolution. Geological Journal, 26(1), pp.65-83.
1537	https://doi.org/10.1002/gj.3350260105
1538	Sømme, T. O., Helland-Hansen, W., Martinsen, O. J., Thurmond, J.B. (2009) Relationships between
1539	morphological and sedimentological parameters in source-to-sink systems: a basis for
1540	predicting semi-quantitative characteristics in subsurface systems. Basin Research. 21, 361-
1541	387. https://doi.org/10.1111/j.1365-2117.2009.00397.x
1542	Strong, G.E. and Milodowski, A.E., 1987. Aspects of the diagenesis of the Sherwood Sandstones of
1543	the Wessex Basin and their influence on reservoir characteristics. Geological Society, London,
1544	Special Publications, 36(1), pp.325-337. https://doi.org/10.1144/GSL.SP.1987.036.01.23
1545	Sumbler, M G, Barron, A J M, and Morigi, A N. 2000. Geology of the Cirencester district. Memoir of the
1546	British Geological Survey, Sheet 235 (England and Wales).
1547	Svendsen, J.B. and Hartley, N.R., 2001. Comparison between outcrop-spectral gamma ray logging
1548	and whole rock geochemistry: implications for quantitative reservoir characterisation in

1549	continental sequences. Marine and Petroleum Geology, 18(6), pp.657-670.
1550	https://doi.org/10.1016/S0264-8172(01)00022-8
1551	Thomas, L.P.; Holliday, D.W. 1982 Southampton no.1 (Western Esplanade) geothermal well:
1552	geological well completion report. Institute of Geological Sciences, 41pp. (WA/KB/82/003)
1553	(Unpublished)
1554	Thompson, D.B., 1970a. The stratigraphy of the so-called Keuper Sandstone Formation (Scythian–?
1555	Anisian) in the Permo-Triassic Cheshire Basin. Quarterly Journal of the Geological
1556	Society, 126(1-4), pp.151-181. https://doi.org/10.1144/gsjgs.126.1.0151
1557	Thompson, D.B., 1970b. Sedimentation of the Triassic (Scythian) red pebbly sandstones in the
1558	Cheshire Basin and its margins. <i>Geological Journal</i> , 7(1), pp.183-216.
1559	https://doi.org/10.1002/gj.3350070111
1560	Thompson, J. and Meadows, N.S., 1997. Clastic sabkhas and diachroneity at the top of the Sherwood
1561	Sandstone Group: East Irish Sea Basin. Geological Society, London, Special
1562	Publications, 124(1), pp.237-251. https://doi.org/10.1144/GSL.SP.1997.124.01.15
1563	Tyrrell, S., Haughton, P.D., Souders, A.K., Daly, J.S. and Shannon, P.M., 2012. Large-scale, linked
1564	drainage systems in the NW European Triassic: insights from the Pb isotopic composition of
1565	detrital K-feldspar. Journal of the Geological Society, 169(3), pp.279-295.
1566	https://doi.org/10.1144/0016-76492011-104
1567	Underhill, J. and Stoneley, R., 1998, Introduction to the development, evolution and petroleum
1568	geology of the Wessex Basin, Geological Society Special Publications, vol. 133, pp. 1-18.
1569	https://doi.org/10.1144/GSL.SP.1998.133.01.01
1570	Walsh, P.T., Banks, V.J., Jones, P.F., Pound, M.J. and Riding, J.B., 2018. A reassessment of the
1571	Brassington Formation (Miocene) of Derbyshire, UK and a review of related hypogene karst
1572	suffosion processes. Journal of the Geological Society, 175(3), pp.443-463.
1573	https://doi.org/10.1144/jgs2017-029
1574	Walsh, P.T., Collins, P., Ijtaba, M., Newton, J.P., Scott, N.H. and Turner, P.R., 1980. Palaeocurrent
1575	directions and their bearing on the origin of the Brassington Formation (Miocene-Pliocene) of
1576	the southern Pennines, Derbyshire, England, Mercian Geologist, 8(1), pp.47-61

1577	Warrington, G., 1970a. The "Keuper" Series of the British Trias in the northern Irish Sea and
1578	neighbouring areas. <i>Nature</i> , 226(5242), pp.254-256. https://doi.org/10.1038/226254a0
1579	Warrington, G., 1970b. The stratigraphy and palaeontology of the 'Keuper' Series of the central
1580	Midlands of England. Quarterly Journal of the Geological Society, 126(1-4), pp.183-223.
1581	https://doi.org/10.1144/gsjgs.126.1.0183
1582	Warrington, G. and Ivimey-Cook, H.C., 1992. Triassic. In: Cope, J.C.W., Ingham, J.K. & Rawson, P.F.
1583	(eds) Atlas of Palaeogeography and Lithofacies. Memoirs of the Geological Society of London,
1584	13, 97-106. https://doi.org/10.1144/GSL.MEM.1992.013.01.11
1585	Warrington, G. and Pollard, J.E., 2021. On the records of the brachiopod 'Lingula'and associated
1586	fossils in Mid-Triassic deposits in England. Proceedings of the Yorkshire Geological
1587	Society, 63(4), pp.pygs2020-015. https://doi.org/10.1144/pygs2020-015
1588	Wills, L. J. (1956). Concealed coalfields: a palaeographical study of the stratigraphy and tectonics of
1589	mid-England in relation to coal reserves. London: Blackie.
1590	Wills, L.J., 1970. The Triassic succession in the central Midlands in its regional setting. Quarterly
1591	Journal of the Geological Society, 126(1-4), pp.225-283.
1592	https://doi.org/10.1144/gsjgs.126.1.0225
1593	Wills, L. J. (1976). The Trias of Worcestershire and Warwickshire. Report (Institute of Geological
1594	Sciences (Great Britain)), 76/2. London : HMSO.
1595	Wilson, A.A., 1990. The Mercia Mudstone Group (Trias) of the East Irish Sea Basin. Proceedings of
1596	the Yorkshire Geological Society, 48(1), pp.1-22. https://doi.org/10.1144/pygs.48.1.1
1597	Wilson, A. A., 1993. The Mercia Mudstone Group (Trias) of the Cheshire Basin. Proceedings of the
1598	Yorkshire Geological Society, 49(3), pp.171-188. https://doi.org/10.1144/pygs.49.3.171
1599	Wilson, A. A. and Evans, W. B. 1990. Geology of the country around Blackpool. <i>Memoir of the British</i>
1600	Geological Survey, Sheet 66 (England and Wales).
1601	Wrobel-Daveau, J., Nicoll, G., Tetley, M. G., Gréselle, B., Perez-Diaz, L., Davies, A. & Eglington, B. M.
1602	(2022) Plate tectonic modelling and the energy transition. Earth-Science Reviews. 234,
1603	104227. https://doi.org/10.1016/j.earscirev.2022.104227

1604	Yu9824, 2021. Ternary Diagram. https://github.com/yu9824/ternary-diagram/ . Accessed 28 th
1605	November 2024
1606	Zuffa, G.G., 1985. Optical Analyses of Arenites: Influence of Methodology on Compositional Results.
1607	In: Zuffa, G.G. (ed) Provenance of Arenites. NATO ASI Series, vol 148. Springer, Dordrecht.
1608	https://doi.org/10.1007/978-94-017-2809-6_8
1609	

Table 1: List of commonly abbreviated stratigraphic and paleogeographic terms used in text.

Abbreviation	Full name
CHF	Chester Formation (Sherwood Sandstone Group)
EISB	East Irish Sea Basin
EMS	East Midlands Shelf
HSF	Helsby Sandstone Formation (Sherwood Sandstone Group)
LBM	London-Brabant Massif
MMG	Mercia Mudstone Group
MTU	Mid-Triassic Unconformity (former Hardegsen Unconformity)
SMF	Sidmouth Mudstone Formation (Mercia Mudstone Group)
SSG	Sherwood Sandstone Group
TSF	Tarporley Siltstone Formation (Mercia Mudstone Group)
WSF	Wilmslow Sandstone Formation (Sherwood Sandstone Group)

Table 2: Key sedimentological parameters for the Helsby Sandstone Formation (HSF) in each sedimentary basin in the mapped fairway (**fig. 3**). Median porosities compiled by Medici et al. (2019a), except the Wessex Basin (estimated from Bowman et al., 1993; Newell and Shariatipour, 2016). Estimated proportion of fluvial and aeolian deposits compiled from Thompson et al. (1970), Meadows and Beach (1994b), McKie et al. (1997), Ambrose et al. (2014), Newell (2018b).

Basin	Wessex	Worcester	Midlands	Cheshire	East Irish Sea
Median porosity (%)	18.0	14.8	26.9	24.0	12.7
Proportion of fluvial deposits (%)	90	100	100	71	64
Proportion of aeolian deposits (%)	10	0	0	29	36

Table 3: Summary statistics for petrographic data within the Helsby Sandstone Formation (HSF), grouped by study, by point count method (Augustsson et al., 2021), and by basin.

	Point count method	Wessex Basin (W)	Wessex Basin (E)	Worcester Graben	Midlands Basins	Cheshire Basin	East Irish Sea Basin
Meadows,							
pers comms.	Traditional					10	121
De Sainz Simpson, 2022	Gazzi- Dickinson					41	44
Scorgie et al., 2021	Traditional						12
Svendsen and Hartley, 2001	Gazzi- Dickinson	23					
Chisholm et al., 1988	Unknown						
Burley, 1987	Traditional	9	11			11	18
Knox et al., 1984	Gazzi – Dickinson		14				
Ali et al., 1982	Unknown				5		

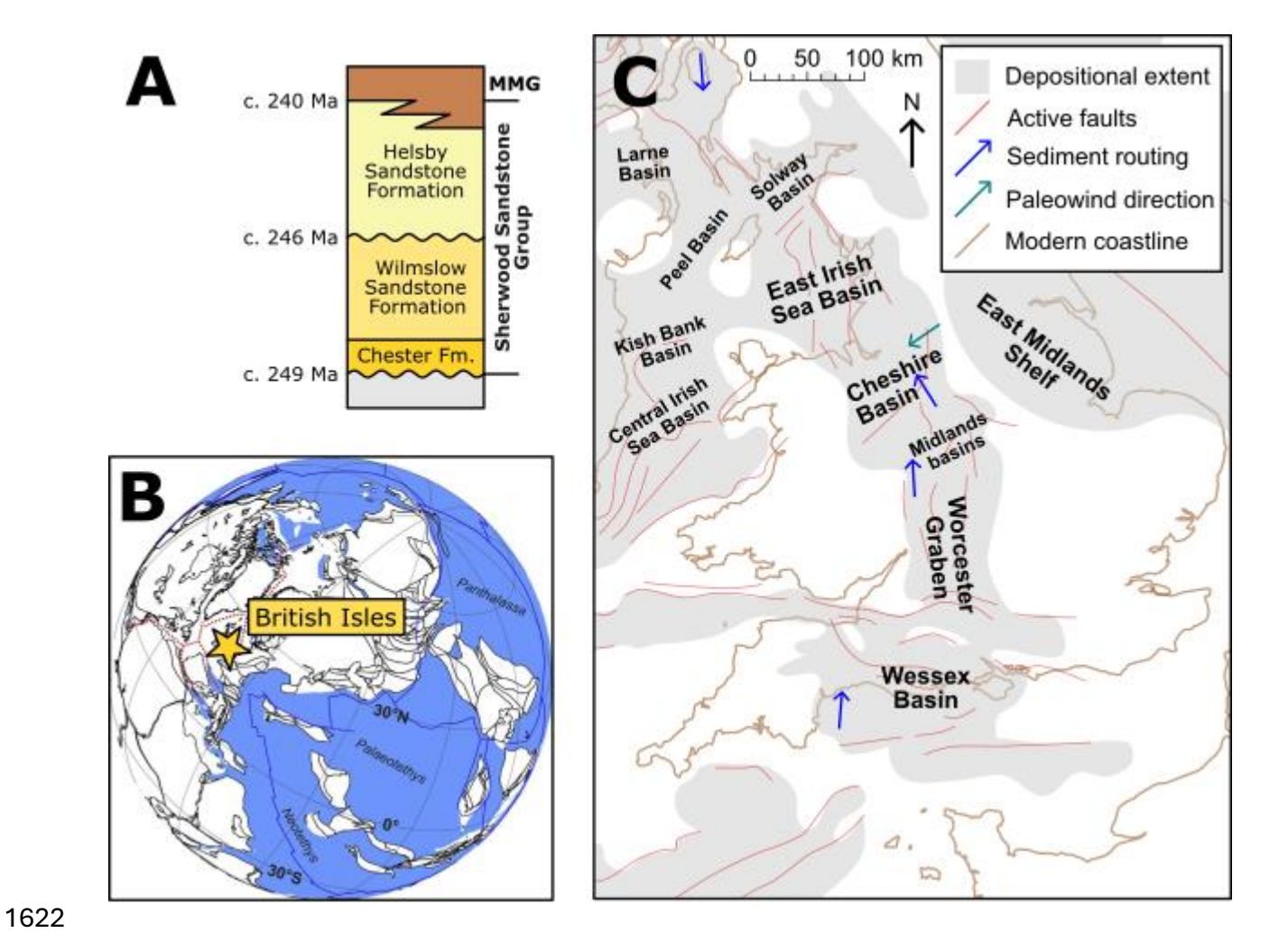
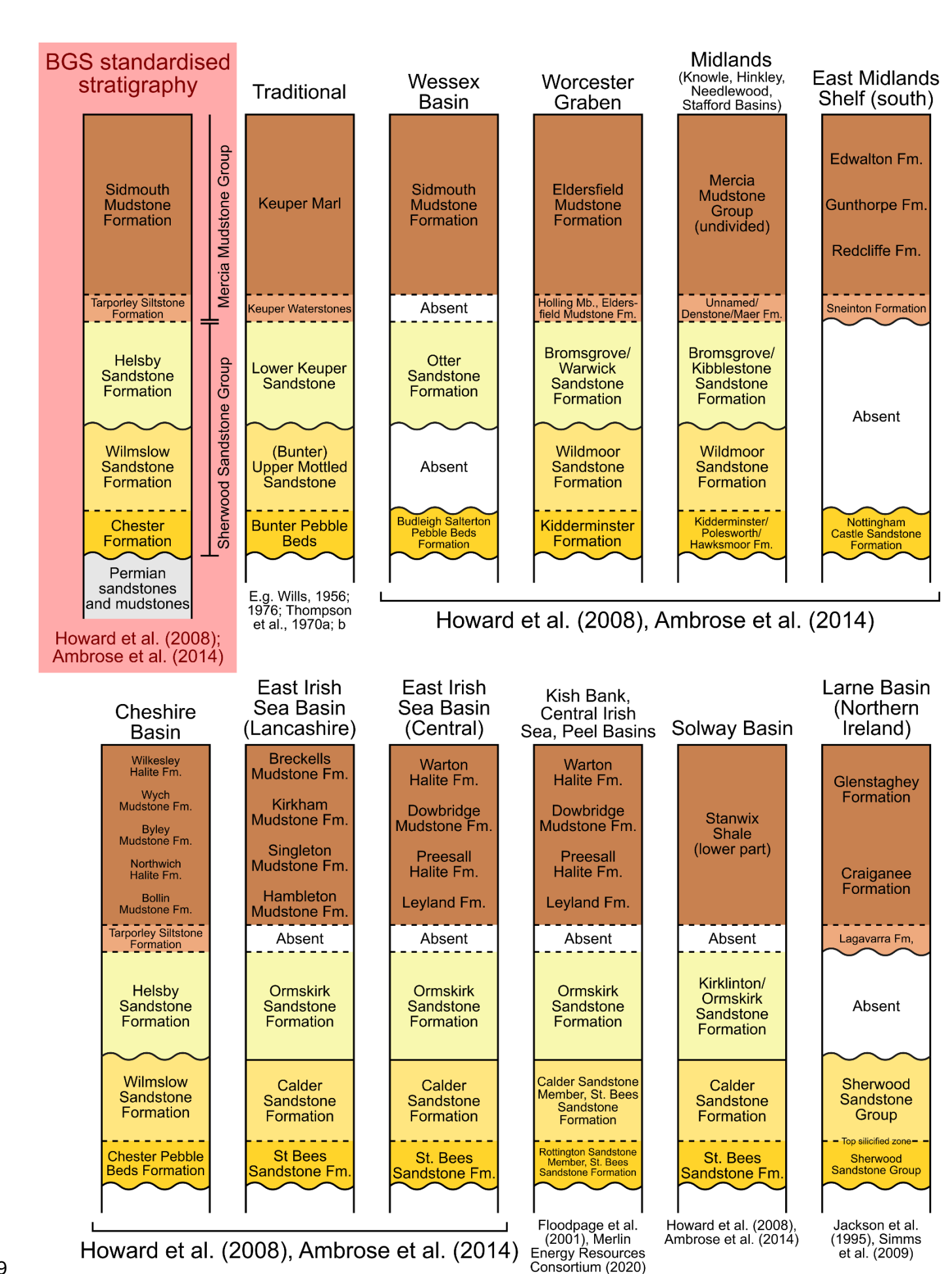


Figure 1: (a) General stratigraphy (Ambrose et al., 2023) and ages (Hounslow and McIntosh, 2003; Hounslow and Gallois, 2023) of the lower and middle Triassic succession of the British Isles, comprising the Sherwood Sandstone Group and Mercia Mudstone Group (MMG). **(b)** Global position of the British Isles during the lower Triassic, adapted from Newell (2017a). **(c)** General basin configuration of the British Isles during the mid-Triassic. Adapted from Warringon and Ivimey-Cook (1992).



1630	Figure 2: Commonly used regional lithostratigraphic terms for the Sherwood Sandstone Group
1631	and Mercia Mudstone Group correlated to the BGS revised, standardised stratigraphy in Britain.
1632	See Ambrose et al. (2014) and Howard et al. (2008) for a comprehensive review of SSG and MMG
1633	regional terminology, respectively.

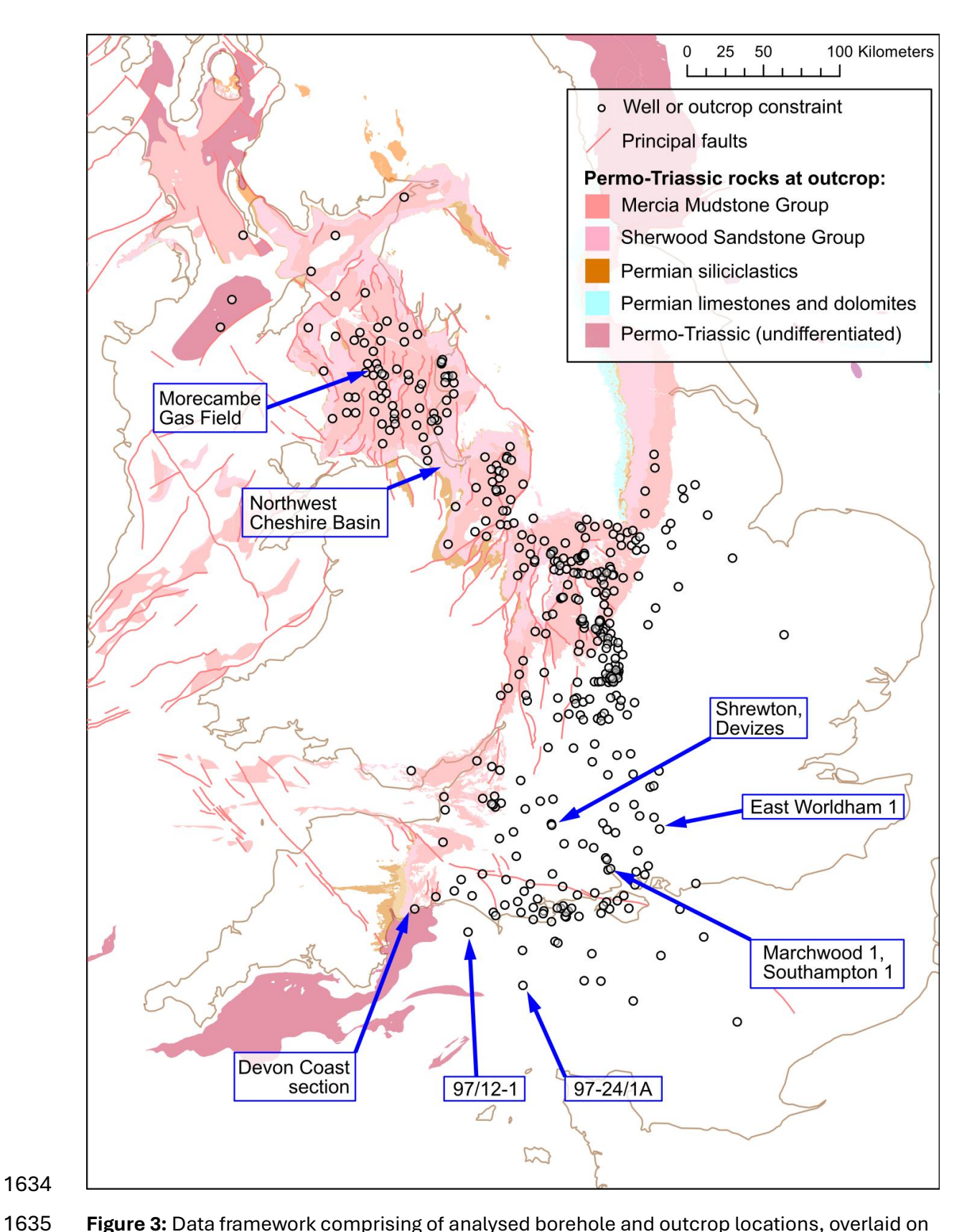


Figure 3: Data framework comprising of analysed borehole and outcrop locations, overlaid on Permo-Triassic outcrop geology and structure of the British Isles. Labelled wells and outcrop are mentioned in the text. Geological Map Data BGS © UKRI 2025

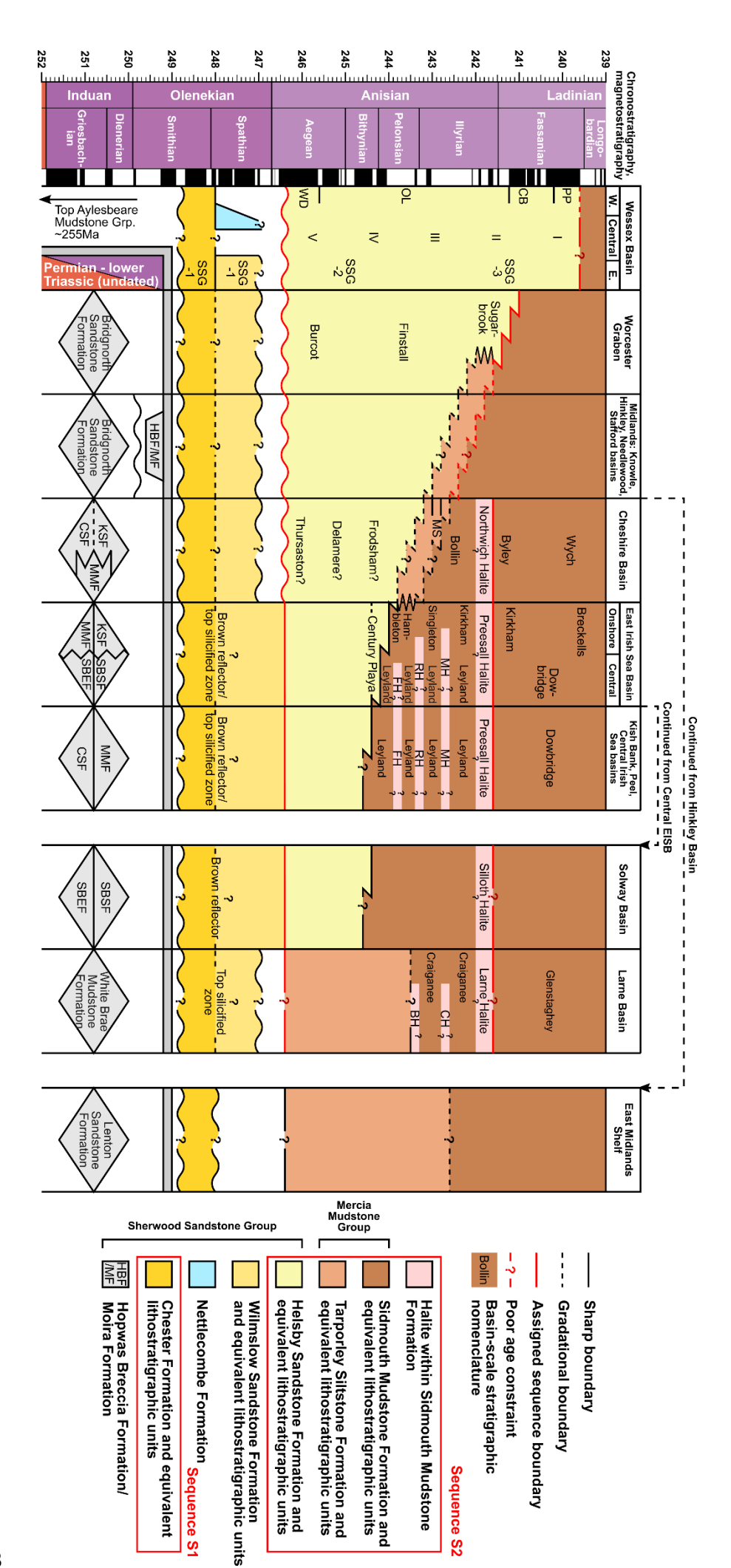


Figure 4: Integrated litho- and chronostratigraphic correlation for the Permian to middle Triassic System in the British Isles, including undated Permo-Triassic units, the Sherwood Sandstone Group (SSG) and lower Mercia Mudstone Group (MMG). Basins are ordered from southeast to northwest. Chronostratigraphic and magnetostratigraphic timescale adapted from Ogg et al. (2020). PP: Pennington Point Member, CB: Chiselbury Bay Member, OL: Otterton Ledge Member, WD: West Down Member, MS: Malpas Sandstone Member, MH: Mythrop Halite Member, RH: Rossall Halite Member, FH: Fylde Halite Member, CH: Carnduff Halite Member, BH: Ballybolley Halite Member, KS: Kinnerton Sandstone Formation, MMF: Manchester Marls Formation, CSF: Collyhurst Sandstone Formation, SBSF: St Bees Shale Formation, SBEF: St Bees Evaporites Formation

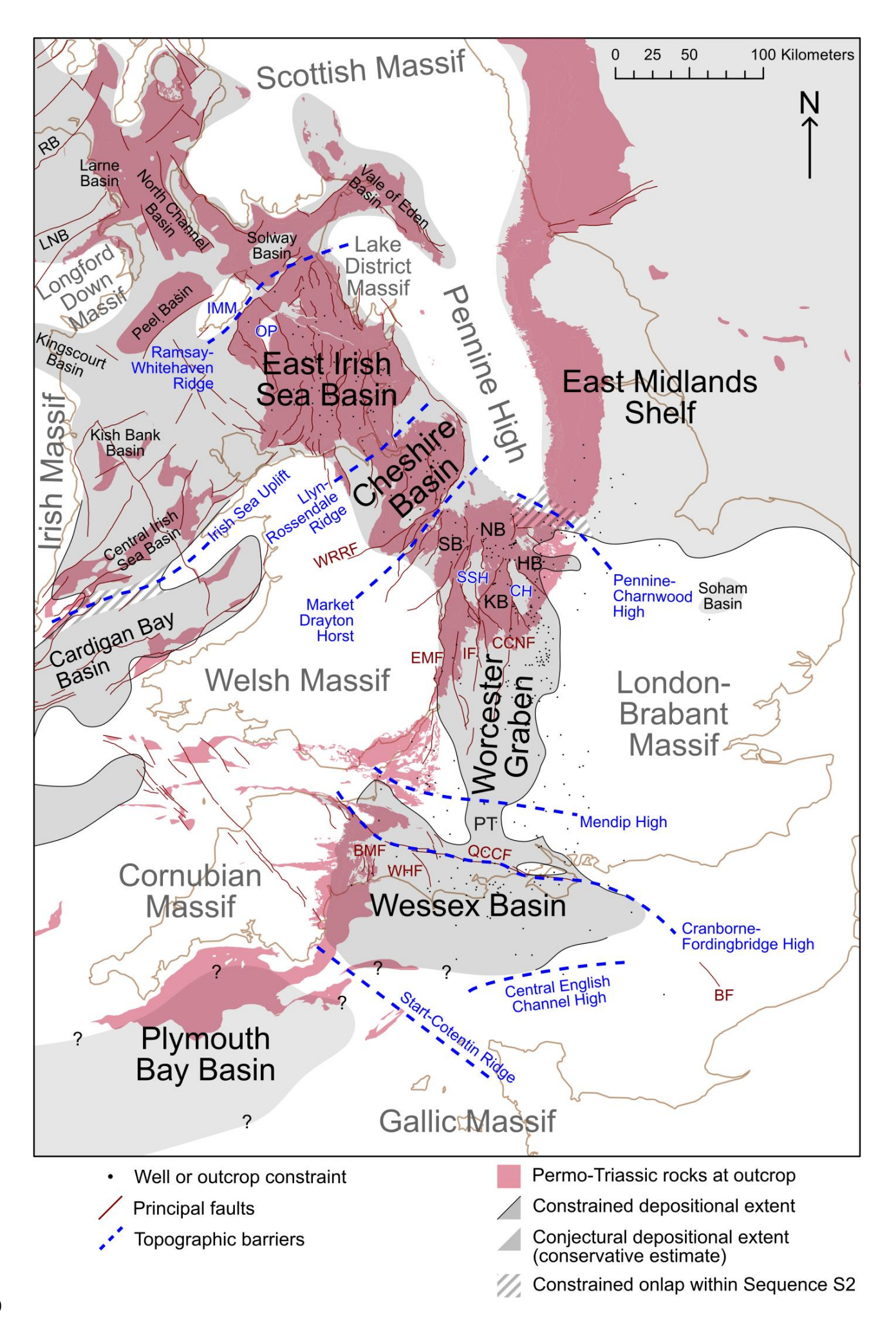


Figure 5: Structural and palaeogeographic setting during Sequence S2 (middle Triassic) in the British Isles. Depositional extents outside borehole-constrained areas from Jackson et al. (1995), Dunford et al. (2001); Simms et al. (2009) and McKie (2017). Structures adapted from BGS and Newell (2018). BF: Bray Fault; BMF: Beer-Musbury Fault; CH: Coventry Horst; CCNF: Clopton-Clapton-Northleach Fault; EMF: East Malvern Fault; HB: Hinkley Basin; IF: Inkerberrow Fault; IMM: Isle of Man Massif; KB: Knowle Basin; LNB: Lough Neagh Basin; NB: Needlewood Basin; OP: Ogham Platform; PT: Pewsey Trough; QCCF: Quantocks-Coker-Cranborne Fault; RB: Rathlin Basin; SB: Stafford Basin; SSH: South Staffordshire Horst; WRRF: Wem-Red Rock Fault. Geological Map Data BGS © UKRI 2025

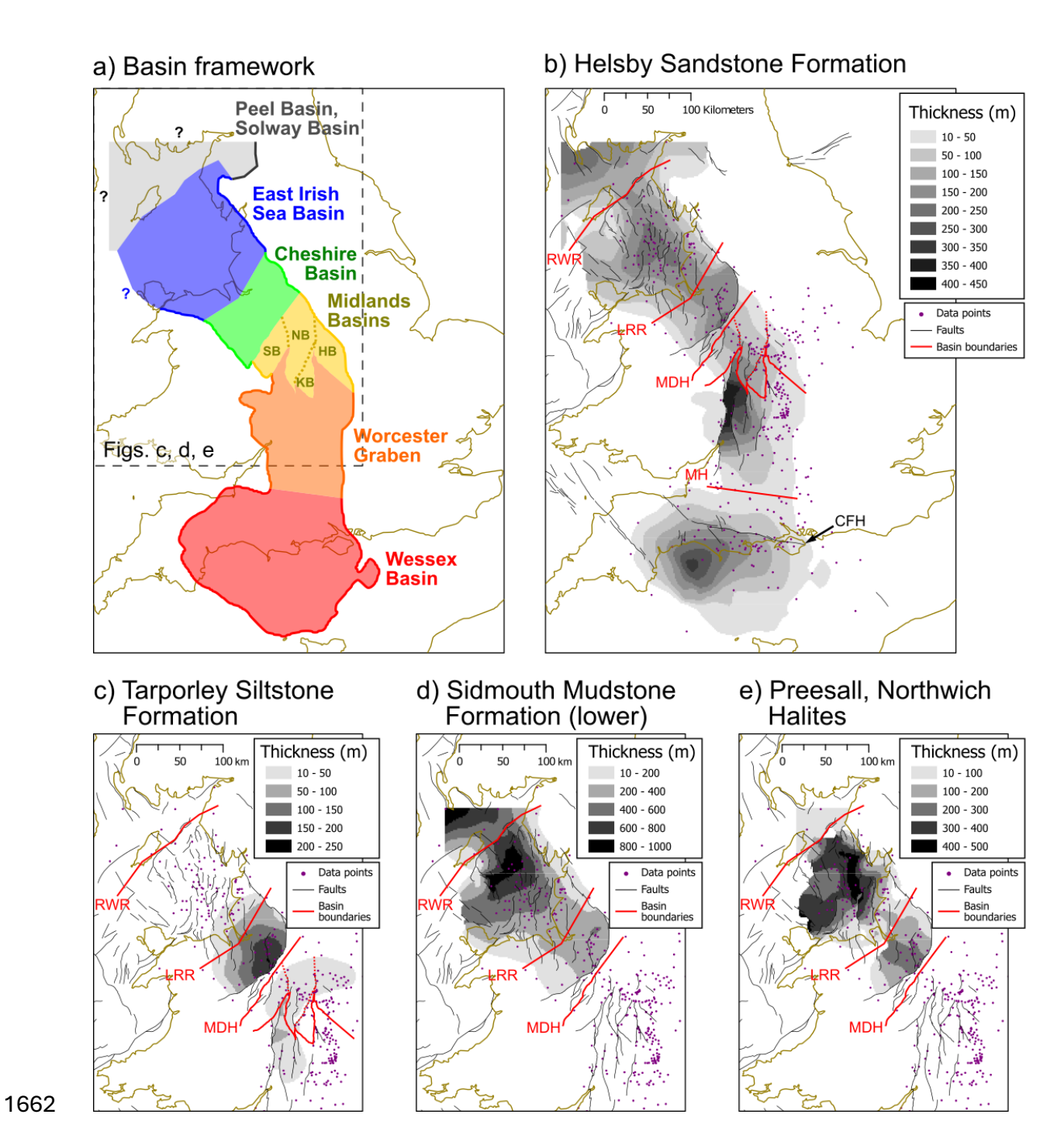


Figure 6: a) Basin configuration for the isopach maps of the studied lithostratigraphic units. Isopach maps for the: **b)** Helsby Sandstone Formation (HSF), Sherwood Sandstone Group (SSG), **c)** Tarporley Siltstone Formation (TSF), Mercia Mudstone Group (MMG), **d)** Sidmouth Mudstone Formation (SMF), MMG (below but excluding the Preesall and Northwich Halites), **e)** Preesall and Northwich Halites, MMG. SB: Stafford Basin, NB: Needlewood Basin, HB: Hinkley Basin, KB: Knowle Basin. CFH: Cranborne-Fordingbridge High, MH: Mendip High, MDH: Market Drayton Horst, LRR: Llyn-Rossendale Ridge, RWR: Ramsay-Whitehaven Ridge.

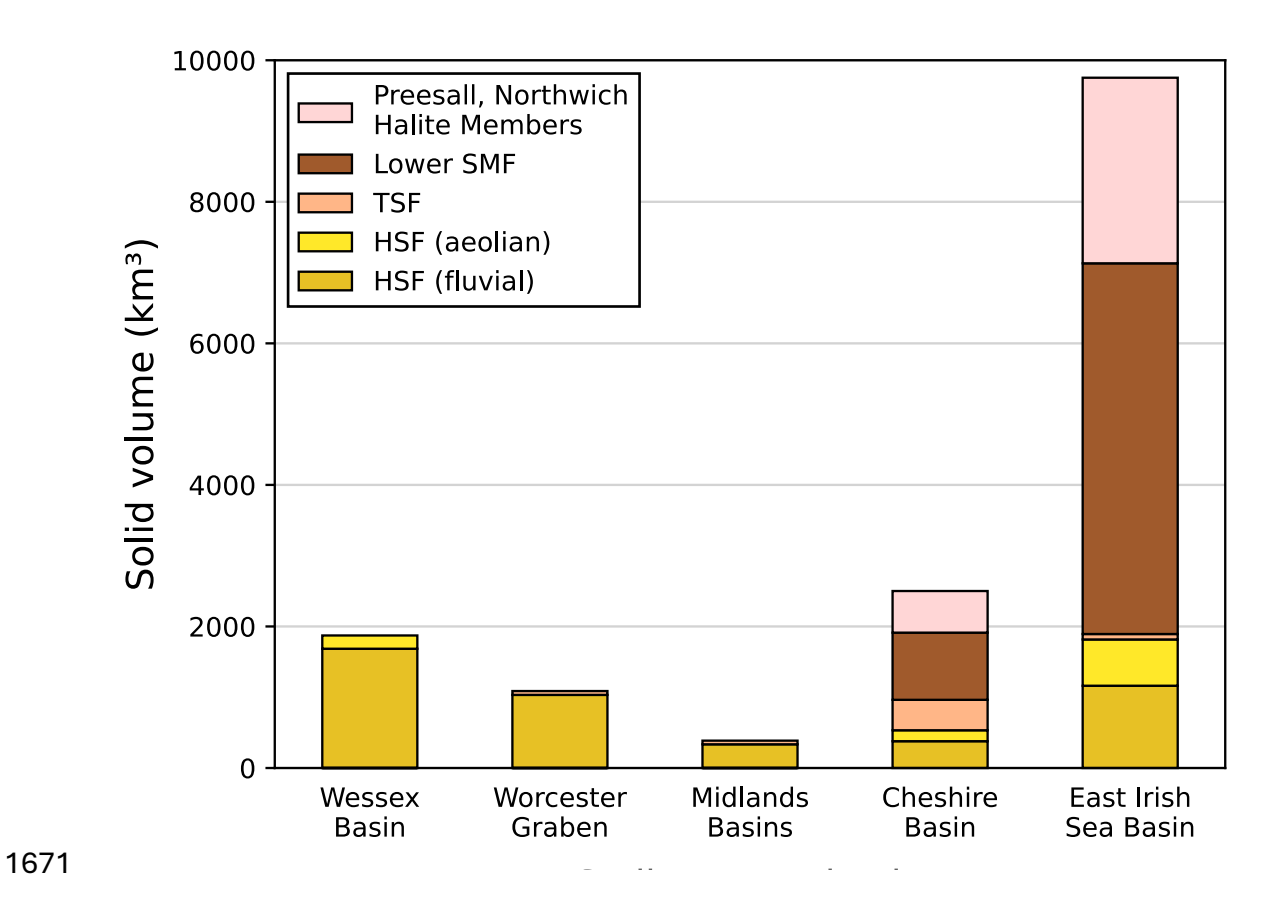
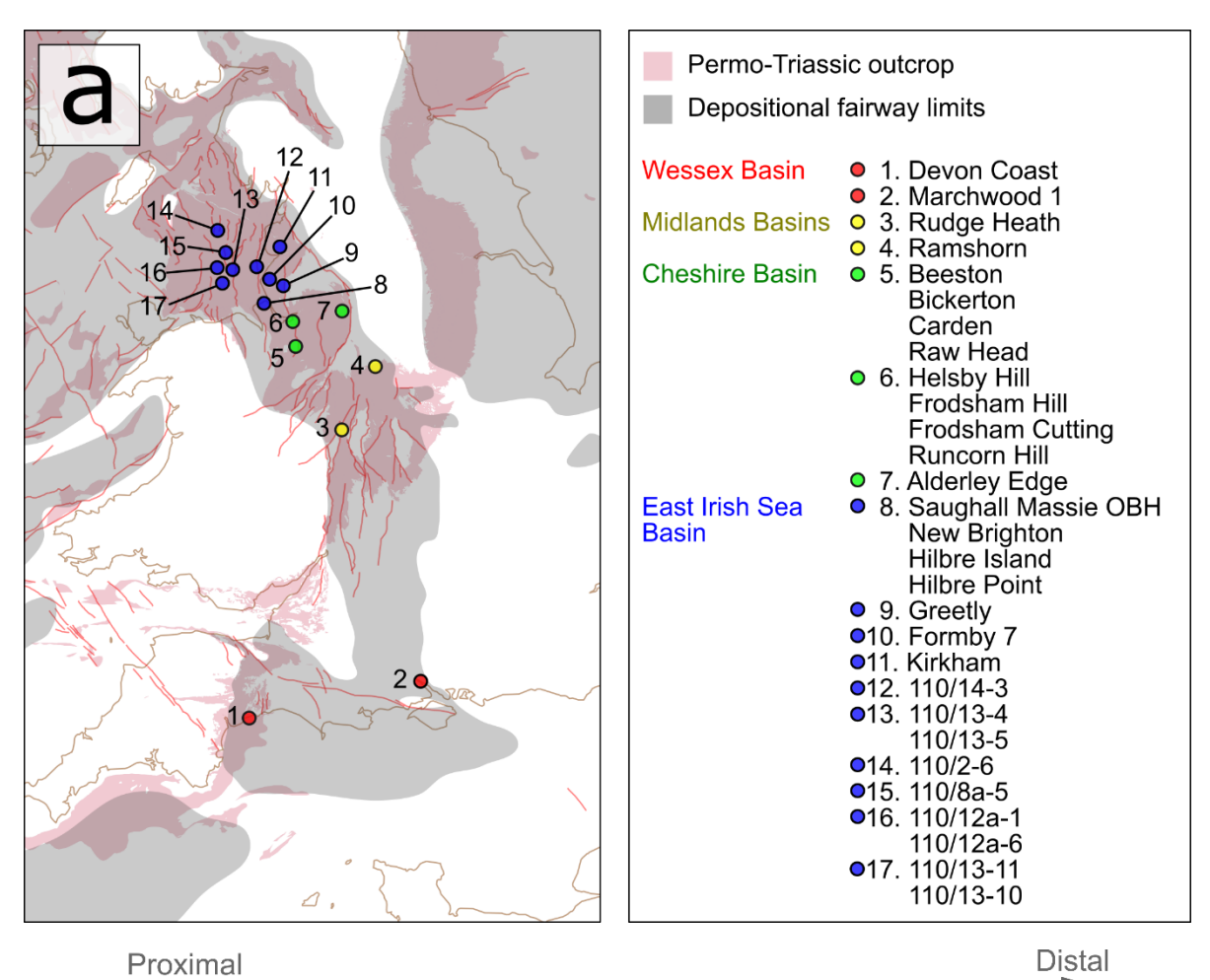


Figure 7: Solid rock (porosity removed) sediment volumes for the basins within Sequence S2 (**fig. 2**), arranged downsystem (south to north) between the Wessex Basin and the EISB (**fig. 6**). Solid rock sediment volumes are divided by respective lithostratigraphic units, and within the Helsby Sandstone Formation (HSF), by aeolian and fluvial deposits. TSF: Tarporley Siltstone Formation, SMF: Sidmouth Mudstone Formation.



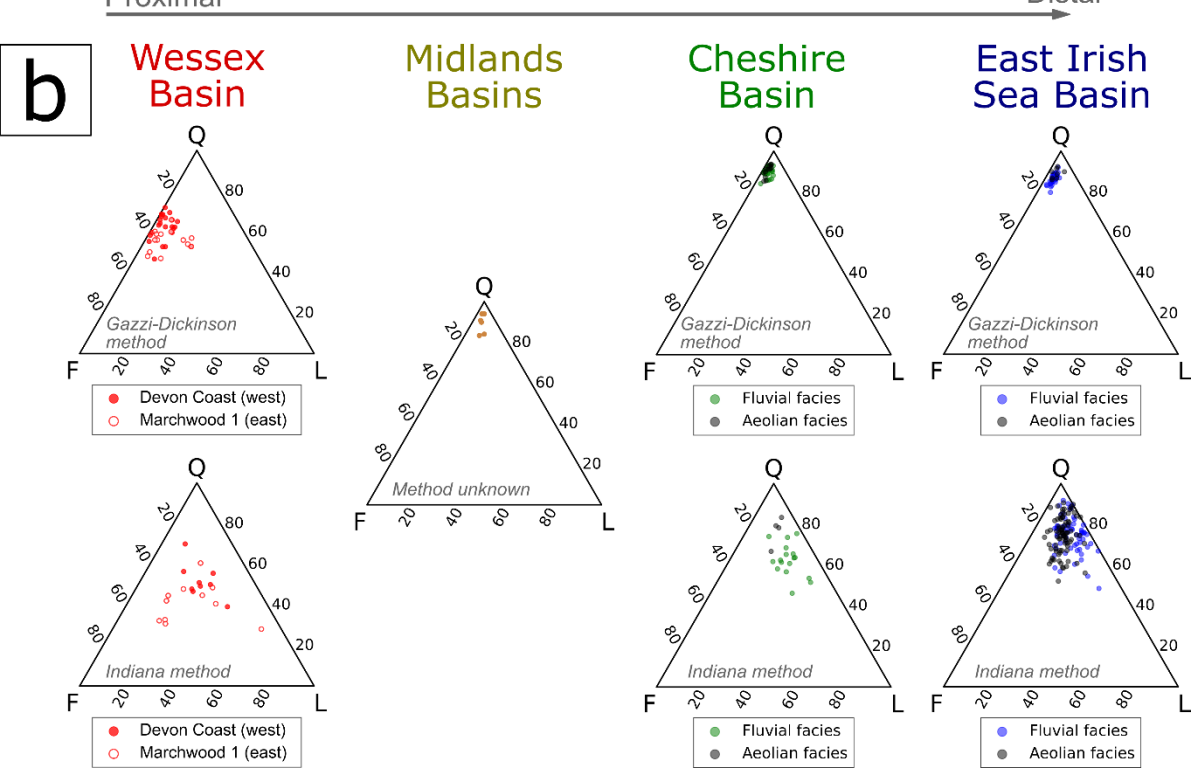


Figure 8: a) Map showing localities within the Helsby Sandstone Formation (HSF) where sandstone bulk petrographic data has been documented, divided by sedimentary basin

1681	(Knox et al., 1984; Burley, 1987; Ali, 1983; Chisholm et al., 1988; Scorgie et al., 2021; De
1682	Sainz Simpson, 2022; Meadows, pers. comm). Geological Map Data BGS © UKRI 2025 b)
1683	Sandstone QFL plots for each basin area in the HSF, divided by point count method. Bulk
1684	mineralogical data is also divided between fluvial and aeolian deposits in the Cheshire
1685	Basin and EISB. Ternary diagrams plotted using Ternary-Diagram (Yu9824, 2021).

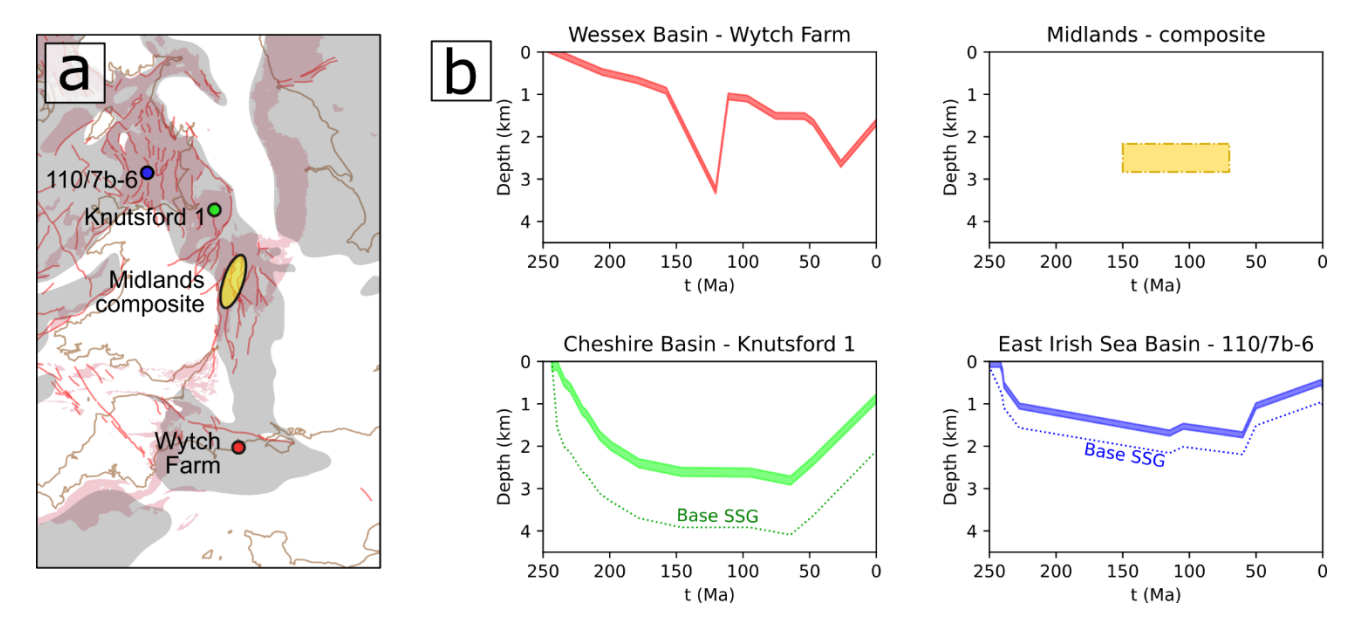


Figure 9: a) Map showing selected localities where burial histories for the Helsby Sandstone Formation (HSF) have been reconstructed from vitrinite reflectance and apatite fission track analysis. Geological Map Data BGS © UKRI 2025 **b)** Representative diagenetic histories for each basin, taken at the Wytch Farm oilfield for the Wessex Basin (Bray et al., 1998), a composite of wells in the western part of the Midlands Basins (Carter et al., 1995), well Knutsford 1 in the Cheshire Basin (Mikkelsen and Floodpage, 1997), and well 110/7b-6 in the EISB (Gent, 2006).

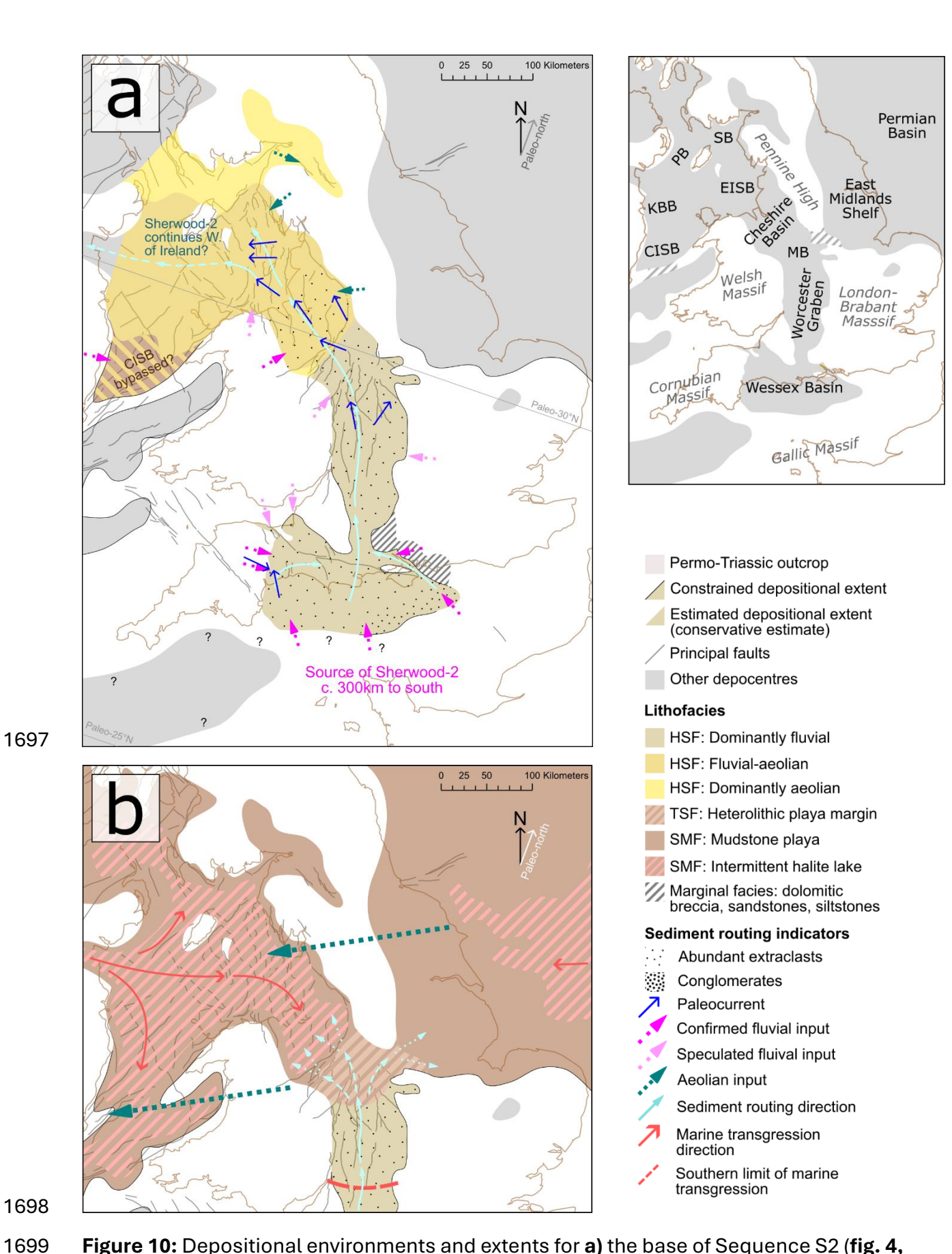


Figure 10: Depositional environments and extents for **a)** the base of Sequence S2 (**fig. 4,** Helsby Sandstone Formation, HSF), and **b)** the top of Sequence S2 in the northern portion of the fairway (**fig. 4,** HSF, Tarporley Siltstone Formation (TSF), lower Sidmouth Mudstone

Formation (SMF)). Confirmed and speculated sediment inputs (Wills, 1956; 1976; Warrington and Ivimey-Cook, 1970; Smith and Edwards 1991; Jones and Ambrose, 1994; Mountney and Thompson, 2002; Tyrrell et al., 20125; Morton et al., 2013; 2016; Marsh et al., 2022), representative palaeocurrent measurements (Thompson, 1970b; Chisolm et al., 1988; Smith and Edwards, 1991; Old et al., 1987; 1991; Herries and Cowan, 1997; Newell, 2017) and first-order grain size changes are shown. Palaeogeography and fairway framework follows **fig. 5** and references therein. Palaeo-north and palaeolatitude from Dercourt et al. (2000). ESIB: East Irish Sea Basin, CISB: Central Irish Sea Basin, KBB: Kish Bank Basin, MB: Midlands Basins, PB: Peel Basin, SB: Solway Basin. **(a, b)** Geological Map Data BGS © UKRI 2025

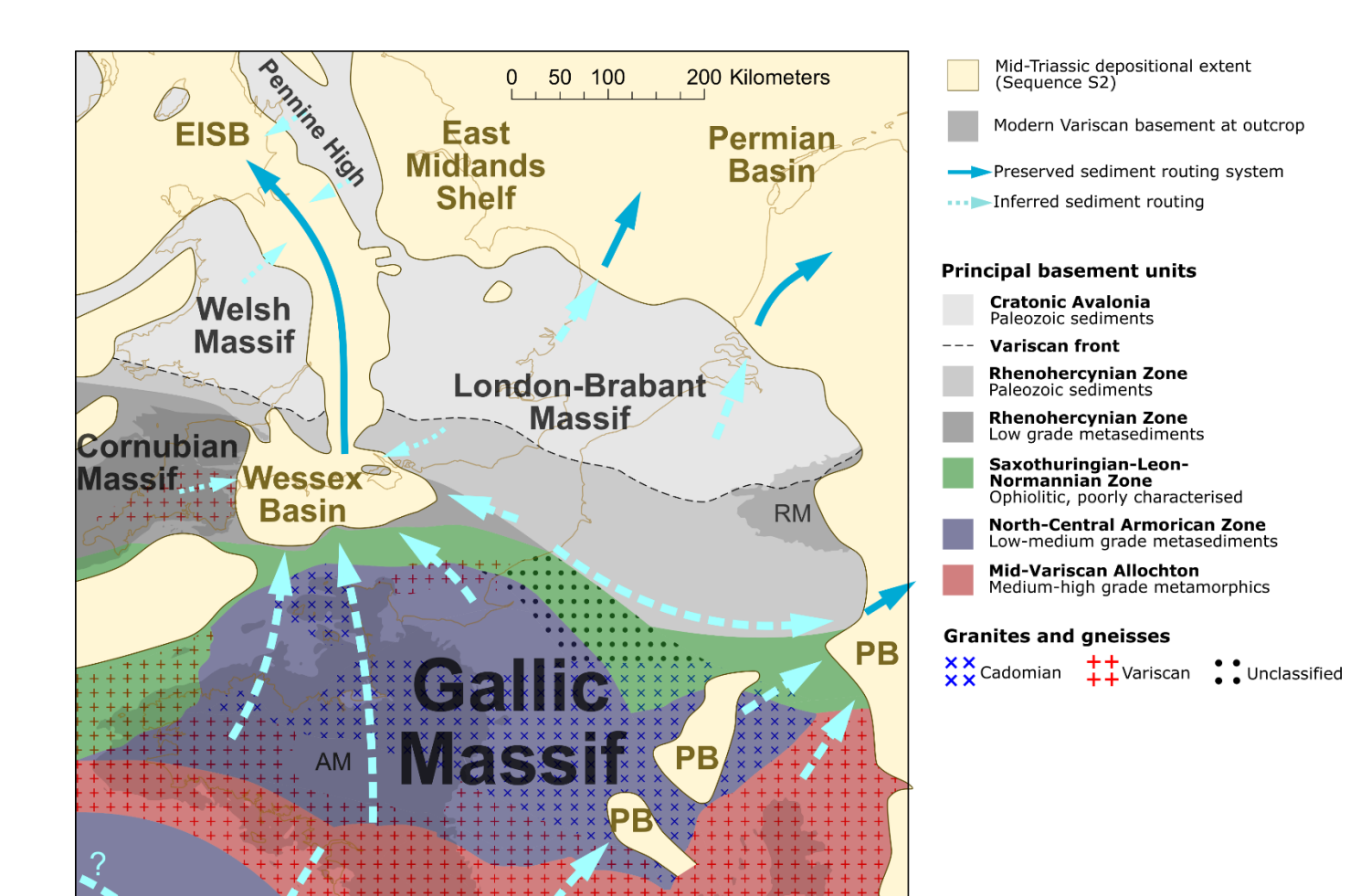


Figure 11: Triassic sedimentary basins and sediment routing in northwest Europe superimposed on a map of first-order Variscan tectonic units. UK basins from fig. 5, and references therein. Other basins from Bourquin et al. (2006), McKie et al. (2017), and Ceccetti et al. (2024). Basin and sediment routing configuration is portrayed for the mid-Anisian. AM: Armorican Massif, MC: Massif Central, RM: Rhenish Massif. BR: Biscay Rift, PB: Paris Basin. Basement lithologies for continental Europe adapted from Megnien (1980), Baptiste (2016), Laurent et al. (2021) and Catalán et al. (2021). Basement lithologies for the English Channel area adapted from Hamblin et al. (1992), Shail and Leveridge (2009) and Baptiste (2016). Basement lithologies for the UK adapted from Shail and Leveridge (2009); Butler (2018), and Pullan and Donato (2022)